Title

Annotating Hypothetical Proteins in *Escherichia coli* K-12

Author information

Sagarika Chakraborty[1], Zachary Ardern[1,2], Habibu Aliyu[1] and Anne-Kristin Kaster[1,3]*

[1] Institute for Biological Interfaces 5 (IBG-5), Biotechnology and Microbial Genetics, Karlsruhe Institute of Technology (KIT), Hermann-von-Helmholtz-Platz 1, 76344 Eggenstein-Leopoldshafen, Germany

[2] Wellcome Trust Sanger Institute, Hinxton, Saffron Walden CB10 1RQ, United Kingdom

[3] Institute for Applied Biosciences (IAB), Karlsruhe Institute of Technology (KIT), Kaiserstraße 12, 76131 Karlsruhe, Germany

* To whom correspondence should be addressed: Email: kaster@kit.edu

Graphical Abstract

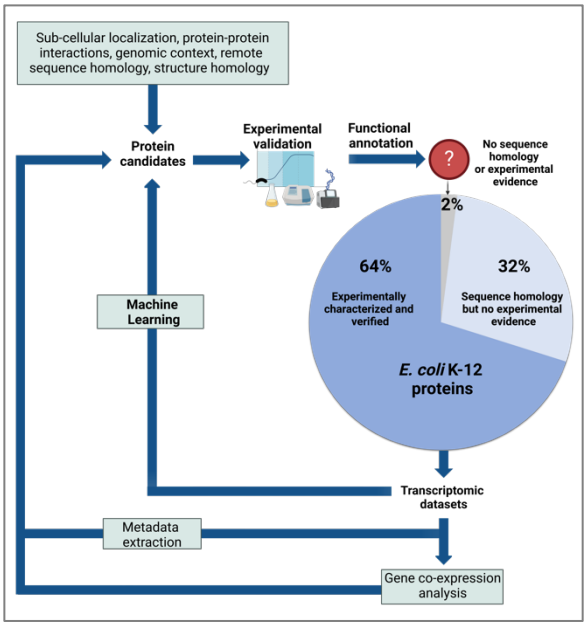

Abstract

Omics technologies have led to the discovery of a vast number of proteins that are expressed but have no functional annotation - so called hypothetical proteins (HPs). Even in the best-studied model organism *Escherichia coli* K-12, over 2% of the proteome remains uncharacterized. This knowledge gap becomes even worse when looking at microbial dark matter. However, knowing the functions of proteins is crucial for elucidating cellular and metabolic processes and harnessing biotechnological potentials. Here, we employed machine learning to decipher the transcriptional regulatory network of *E. coli* K-12, as well as other *in silico* tools to assign functions to uncharacterized HPs. We further provide experimental validation of *in silico* predicted functions for three HP-encoding genes (*yhdN*, *yeaC* and *ydgH*) as proof of concept, by analyzing growth patterns of deletion mutants compared to the wild type, as well as their transcriptional responses to specific conditions. This study demonstrates that the use of Big Omics Data in combination with Artificial Intelligence and experimental controls is a powerful approach to illuminate functional dark matter.

Keywords: Artificial Intelligence / Big Omics Data / Functional Annotation of Proteins / Functional Dark Matter / Independent Component Analysis (ICA)

Introduction

Due to the advents in Next Generation Sequencing technologies, the volume of omics data has massively increased over the past years. As of today, gold-standard knowledgebases like the National Center for Biotechnology Information (NCBI)'s Reference Sequences Database (RefSeq) and the Universal Protein Resource Database (UniProt) [1] provide freely accessible sequences and information for over 163 million unique prokaryotic proteins **(Figure 1)**. This rapid accumulation of sequencing data has long surpassed the rate of possible experimental characterization *in vivo* and *in vitro*. Hence, researchers often rely on functional analysis of proteins from model organisms. These findings are then extrapolated *in silico* to closely related sequence homologues. Consequently, the definition of cut-off values plays a crucial role in protein annotation. To manage this challenge, automated annotation pipelines, such as InterPro have become a valuable tool [2]. Here, analysis of protein sequences is provided by classifying them into families and integrating predictive models from multiple protein databases such as e.g. Pfam [3], ProSite [4], SMART [5] and/or CDD [6] to infer functions for experimentally uncharacterized proteins. However, only 83% of all UniProt sequences have so far been functionally annotated by InterPro [7] The remaining 17% of proteins are designated with terms such as 'putative uncharacterized', 'uncharacterized', 'unknown protein families (UPFs)' or proteins bearing 'domains of unknown functions' (DUFs). These proteins are summarized by the term hypothetical proteins (HPs), since they are expressed but could so far not be functionally characterized by classical *in vivo*, *in vitro*, and/or *in silico* methods (8,9). In addition, there is also no information on these proteins available in widely-used knowledge-databases such as BioCyc [10], RegulonDB [11], and EggNOG [12] **(Figure 1).**

While there have been notable advancements in methodologies for protein function prediction in the recent past [13–16] several challenges persist [17,18]: These include different functionalities across homologous proteins, proteins performing different functions in distinct cellular locations, proteins with multiple three-dimensional structures, the lack of conserved proteins across different species to identify shared functional relationships and a heavy

reliance on pre-existing data for inferential annotations [19]. Even in the best studied model organisms *Escherichia coli* K-12, 31.8% of the genome comprises of protein encoding genes that lack experimental validation, commonly referred to as 'Putative HPs' [8], and 2.1% that even lack sequence homologies (this study) (**Figure 1**). The problem of annotating HPs becomes even larger when looking at microbial dark matter(9, 20).In uncultivated microorganisms, the proportions of genes with unknown functions can comprise up to 60% in bacterial and 80% in archaeal genomes [21]. However, elucidating the function of these proteins is essential for understanding cellular processes, metabolism and evolution, as well as for harnessing their biotechnological potential [22].

Transcriptional profiling has helped to gain insights on protein functions by monitoring gene expressions and clustering genes based on their responses to varying environmental conditions and stimuli [23]. Here, the entire set of RNA transcripts produced by a genome under specific conditions provides a dynamic representation of the organisms' operational state. However, standard bioinformatics-based methods for transcriptomic data analysis are low-throughput and require quite extensive computing power and time due to the high degrees of complexity and heterogeneity of the data [24]. Today, artificial intelligence (AI)-based methodologies have made significant advancements over traditional bioinformatics approaches, offering the capacity to process and analyze data at a scale and speed that were previously unattainable [24, 25]. They are particularly suited for deciphering complex interactions among genes and transcription factors or proteins that regulate them, as well as revealing the regulation of gene expression in response to diverse environmental conditions [27]. Among various techniques for analysis, module-detection methods have proven to efficiently predict the functions of co-regulated groups of genes from large gene expression datasets [28]. Independent Component Analysis (ICA), introduced by Comon in 1994 [29], employs an unsupervised machine learning (ML) approach, categorizing the input data without any prior information. This technique is especially relevant in the context of transcriptomics, where the goal is to understand the complex interplay of gene expression signals and to

85 decipher co-regulated gene sets. ICA therefore allows to reveal the regulatory patterns and
86 activity levels of genes governed by specific regulators (i.e. transcription factors controlling the
87 expression of genes) across diverse experimental conditions, so called transcriptional
88 regulatory networks (TRNs), thereby disclosing the organizational and functional architecture
89 of genes. Expanding upon this, McConn et al. developed a variant of ICA, termed OptICA,
90 which can be applied to large TRNs, analyzing interactions between transcription factors and
91 their target genes. Here, discrete groups of genes are clustered into robust independent
92 components by avoiding over-clustering of datasets (leading to loss of biological information)
93 or under-clustering (leading to too few clusters and a loss of output resolution), and therefore
94 providing an optimal representation of the organism's underlying TRN [27]. This results in
95 revealing independently regulated gene groups, so called iModulon from transcriptomics
96 datasets [29, 30]. iModulons are therefore the data-driven analogs of so-called regulons - sets
97 of genes governed by regulators [30]. The OptICA algorithm along with high-quality RNA-seq
98 data has recently been used to decipher the TRN of *Bacillus subtilis* [32] and *E. coli* [27] to
99 uncover the detailed responses to environmental conditions and genetic perturbations, e.g.
100 deletion mutants. However, these studies focused on the identification of regulons that were
101 not experimentally described before rather than the functional characterization of HPs.
102
103 In order to decipher the function of HP-encoding genes in the *E. coli* K-12 proteome, we
104 adapted the workflow originally designed for *Bacillus subtilis* [32] and analyzed the gene
105 expression data of the *E. coli* K-12 sub-strains MG1655 and BW25113. Functional
106 characterization of HP-encoding genes was inferred by identifying co-regulated genes under
107 the influence of a common regulator from publicly available transcriptomic datasets. This
108 characterization was then further validated by annotating these genes using specific Gene
109 Ontology (GO) categories through the PANTHER tool (Protein ANalysis THrough Evolutionary
110 Relationships) [33]. Additionally, metadata conditions for the transcriptomic datasets were
111 extracted. Furthermore, other *in silico* methods were employed to determine the sub-cellular
112 localization [34], protein-protein interactions (PPIs) [35], genomic context [36] and sequence-

113 based remote homologies [37]. Structural homology information was obtained by using the
114 AlphaFold Protein Structure Database (AFDB) clusters webserver, which is based on a deep
115 learning (DL) method [38].
116
117 Since AI-predicted functions are usually not experimentally verified, raising the possibility of
118 untrue annotations [9], we also provide an experimental validation of three candidate HP-
119 encoding genes (*yhdN*, *yeaC* and *ydgH*). The growth curves and transcriptional responses of
120 *E. coli* K-12 deletion mutants in comparison to the wild-type strain under specific conditions
121 were analyzed, showing that the *in silico* predictions were indeed true. Hence, the here
122 presented pipeline not only facilitates the discovery of previously unidentified regulators, but
123 also sheds light on our understanding of the function of HPs **(Figure 1).**
124

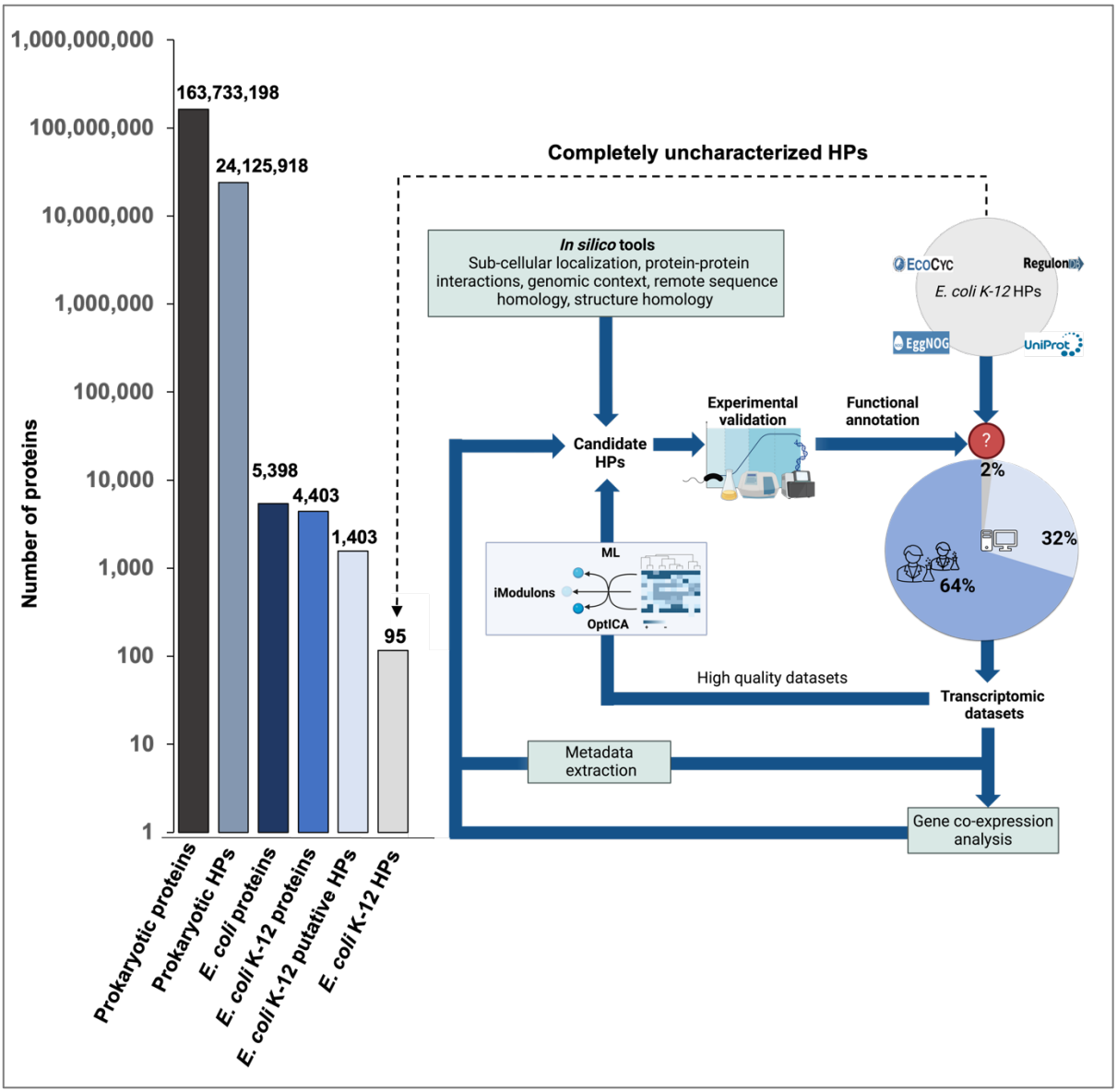

Figure 1. Total number of sequences for all unique prokaryotic and *Escherichia coli* proteins deposited in the National Center for Biotechnology Information (NCBI) as of April 2024 and methodological set-up of this study. Of the 4403 *E. coli* K-12 protein encoding genes, 1403 (31.8%) encode for unique proteins with functions predicted only *in silico* based on homologous sequences but lacking *in vivo* or *in vitro* experimental evidence (termed "putative hypothetical proteins"). 95 protein encoding genes (2.1%) of *E. coli* K-12 are completely uncharacterized with no sequence homologues according to the four knowledge databases - EcoCyc [39], RegulonDB [11], EggNOG [12] and UniProt (1) (termed "hypothetical proteins"). Transcriptomic datasets from NCBI were filtered and processed using the OptICA approach to generate iModulons [32]. Metadata information was curated in parallel using manual or semi-automated approaches(39–41).Bioinformatics, machine learning and deep learning tools along with the presence of relevant metadata then resulted in potential functions for HP candidates for *in vitro* testing. HPs, hypothetical proteins; ICA, independent component analysis; ML, machine learning.

Results and Discussion

143 **Identification of uncharacterized HPs in *E. coli***

144 In 2019, Ghatak et al. had identified HP-encoding genes in *E. coli* K-12, however only by
145 employing keywords such as 'possibly', 'predicted' or 'hypothetical' from the EcoCyc
146 database, or annotation scores of two or below in UniProt [8]. This approach did, however, not
147 establish a stringent threshold for accurate identification of completely uncharacterized HP-
148 encoding genes. Hence, a more rigorous approach was used in this study, which included
149 additional keywords for HPs (such as 'Uncharacterized', 'Putative uncharacterized', 'DUF'
150 etc.) and information on the absence of any functional characterization using multiple gold-
151 standard databases (EcoCyc, UniProt , RegulonDB and EggNOG). 158 of the 1600 HP-
152 encoding genes previously listed by Ghatak et al. have now been functionally characterized
153 with experimental evidence in the EcoCyc database. Notably, the HP-encoding gene *ydfX*,
154 curated as one of the HPs in this study, was missing from Ghatak et al.'s list since it was
155 previously categorized as a pseudogene/phantom gene. Its exclusion, however, could not be
156 verified in the current EcoCyc database. We identified 1403 of 4403 genes (31.8%) of the *E.*
157 *coli* K-12 genome as 'putative' HPs, implying that their functions were inferred based on
158 sequence homologies in the gold-standard databases, but lacking an experimental evidence
159 for function. A recent study using the EggNOG tool also identified about 30% in a different *E.*
160 strain (O157:H7 strain Sakai) as putative HPs [18].

161

162 95 HP-encoding genes (2.1%) could be identified with no sequence homologies in the
163 *E. coli* K-12 genome. These could be further sub-categorized in 'uncharacterized proteins'
164 (53), 'putative uncharacterized' (5), '(DUF)' domain containing proteins (21) and 'UPF' (HPs
165 with unknown protein families, 3). 13 HPs had the characteristic 'Protein Y…' naming scheme.
166 The distribution of those 95 HP-encoding genes within the genome can be found in the
167 Supplementary (*Supplementary Figure 1)*.

168

169

170 **iModulon generation and analysis**

171 In order to investigate the functions for the 95 uncharacterized HP-encoding genes, publicly
172 available RNAseq datasets from *E. coli* K-12 substrain MG1655 were downloaded from NCBI
173 and quality filtered. 779 high-quality datasets from the MG1655 substrain were then used as
174 input for the OptICA algorithm [27]. For the substrain BW25113, a separate OptICA analysis
175 was not conducted due to the very small size of the dataset. The iModulons were identified by
176 utilizing the PyModulon package, specifically employing the *Inferring iModulon Activities*
177 function [32] for the BW25133 substrain. In total, 131 iModulons were obtained for the entire
178 *E. coli* K-12 transcriptome. Three single gene iModulons were discarded from the analyses,
179 since they were considered a result of artificial knockouts or overexpression of single genes
180 in the dataset. Therefore, a total of 128 iModulons were selected for further analysis.
181 Functional information on the HP-encoding genes was obtained by mapping the iModulons to
182 existing experimentally derived regulons (groups of genes regulated by the same transcription
183 factor), using data from the EcoCyc and RegulonDB databases. Additionally, Gene Ontology
184 (GO)-based functional annotations for member genes of an iModulon (co-regulated gene sets)
185 were identified using the PANTHER tool (Protein ANalysis THrough Evolutionary
186 Relationships) [33]. A total of 51 HP-encoding genes were clustered into iModulons using
187 OptICA. Of these, 46 genes were assigned putative functions based on information from
188 regulator proteins and/or Gene Ontology (GO) categories. (**Figure 2**). Two genes, *yfeS* and
189 *yffL* had information on their regulators (RpoE and NarL, respectively) but no assigned GO
190 categories, while five genes (*ybaA, yfaP, yjgZ, ymgI and ymgJ*) (white) could not be associated
191 with a regulator or a GO category. 44 of the HP-encoding genes could not be clustered into
192 distinct iModulons (grey) (**Figure. 2**).
193
194

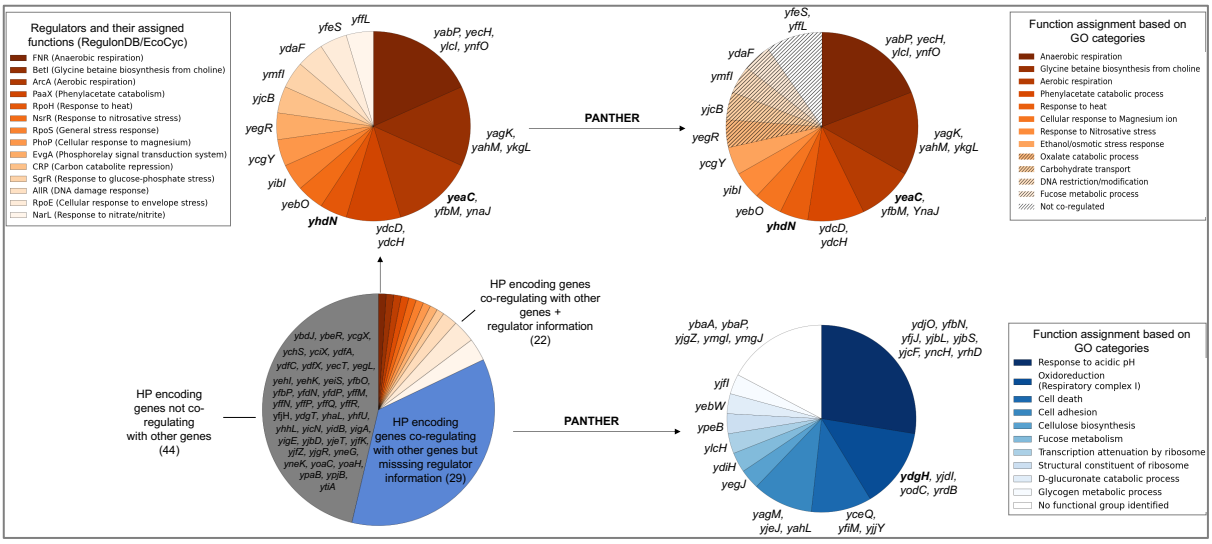

Figure 2. Regulator and functional classification for 95 HP-encoding genes in *Escherichia coli K-12*. 44 HP-encoding genes could not be clustered by the OptICA method [27] (grey), since they did not co-regulate with any other genes. 22 genes were characterized based on information on their regulators as obtained from RegulonDB and/or EcoCyc, as well as by Gene Ontology (GO) categories based on the co-regulating genes using the PANTHER tool (Protein ANalysis THrough Evolutionary Relationships) (orange) [33]. 29 genes co-regulated with other genes, but no information on their regulators could be obtained (blue). 24 out of these 29 genes could be assigned putative functions based on GO annotations of co-regulating genes derived from the PANTHER tool. The striped regions denote genes where the regulator-associated function from EcoCyc/RegulonDB did not match a GO-derived functional category obtained from PANTHER. Highlighted in bold are the three HP-encoding genes which were selected for *in vitro* testing.

In addition to the 95 HP-encoding genes, all other *E. coli K-12* genes were also analysed using this method. 2630 of the 2905 (91%) genes which have experimental evidence of function could also be characterized into iModulons. 1697 (64%) co-regulated with other genes, i.e. they were part of characterized iModulons with information on their regulator on RegulonDB and/or EcoCyc, while 933 of the genes were part of uncharacterized iModulons. For genes with known regulators, only 121 (5%) had either a non-matching functional category when compared with the PANTHER categories or a non-significant (p>0.05) functional category, and 95% had a matching PANTHER GO category. For genes which were part of uncharacterized iModulons, with no regulator information, 546 (58%) could be functionally classified using PANTHER. 1061 of the 1403 putative HP-encoding genes (75%), i.e. genes with functional characterisation based on sequence homology information, could be characterized into iModulons. 342 genes (25%) did not co-regulate with other genes. For genes that had co-regulation, 539 (51%) had information on their regulator on RegulonDB

222 and/or EcoCyc. The other 522 (49%) were part of uncharacterized iModulons. For genes with
223 known regulators, only 20 genes (4%) had either a non-matching function when compared
224 with the PANTHER categories or a non-significant (p>0.05) functional category in PANTHER.
225 For genes with no information on their regulator, 366 (67.9%), could however be characterized
226 by PANTHER. Hence, about 95% of the iModulon functional categories matched the
227 PANTHER GO categories, demonstrating the robustness of the method. Moreover, the
228 inclusion of experimentally characterized genes within uncharacterized iModulons shows
229 potential for the discovery of new regulons or co-regulated genes.
230
231 **Functional analysis of HP-encoding genes using *in silico* tools**
232 All 95 HP-encoding genes were analysed based on multiple criteria including the generated
233 iModulons from the OptICA algorithm, functional information based on the regulators of the
234 co-regulated gene sets obtained *via* RegulonDB/EcoCyc and their GO categories from
235 PANTHER. Information on metadata conditions pertaining to the highest level of gene
236 expression relative to the reference gene *frr* (encoding the ribosome recycling factor) [42] and
237 annotation of the most significant co-expressed gene were also extracted. Additionally, the
238 sub-cellular localization, protein-protein interactions, genomic context, remote sequence
239 homology as well as structural homology aided in forming hypothesises for assigning functions
240 to the respective HPs. 33 of the protein encoding genes (highlighted in green) could be
241 assigned functions with a high confidence. 28 of the genes were assigned functions based on
242 lower confidence, since only information from a maximum of two sources could be well-
243 correlated (highlighted in yellow). A clear inference could not be made for 34 of the genes
244 (highlighted in red). Information retrieved for each gene and functional inference (if applicable)
245 is detailed in **Table1**. A pictorial overview of Table 1 based on the functional annotations for
246 the 95 HPs can be found in *Supplementary Figure 2*.

Table1. A comprehensive functional interference of HPs based on different *in silico* tools. Annotations are based on regulator information from RegulonDB/EcoCyc and/or GO category based on co-regulated genes obtained from PANTHER) [33](as shown in Fig. 2). The highest gene expression condition, obtained from the Tjaden dataset [43], with metadata conditions categorized by the type of medium, oxygen availability (normal O_2 conditions unless stated otherwise), temperature etc. in comparison to the reference gene '*frr'* are described. Functional annotations of co-expressed genes were retrieved from EcoCyc [36]. 'SCL' or sub-cellular localization inferred from the BUSCA tool [34] are abbreviated as either 'NUC' for nuclear 'CYT' for cytoplasmic, 'ECS' for extra cellular space or 'PM' for plasma membrane. Functional information from protein-protein interaction (PPI) analyses was obtained from STRINGdb [35]. Annotations for neighbouring upstream (←) and downstream (→) genes in context of the HP-encoding gene were retrieved from the EcoCyc database. Additionally, remote homology was assessed using the Uniref30 database using the Hhblits tool [37], and structural homology was inferred from the AlphaFold Protein Structure Database [38]. A functional inference can be made for genes supported by multiple lines of evidence when similar functional information was provided by at least two sources. Proteins with well correlated information from at least three sources are highlighted in green (with higher confidence) and proteins with information that can be correlated using at least two sources are highlighted in yellow (with lower confidence). Protein encoding genes highlighted in grey were selected for *in vitro* testing. An unclear inference suggests that, based on the different knowledge bases, the extracted information did not provide enough confidence or could not be well correlated to assign a function (red).

Gene	Function based on regulator and/or co-regulated genes	Condition with highest gene expression (growth medium)	Annotation of most significant co-expressed gene	SCL	PPI: function of partner protein	Annotation of neighbouring genes	Remote homology	Structural homology	Overall functional inference
1. yabP	Anaerobic respiration	M9, 37°C; 100 µg/ml Ampicillin (inhibits cell wall synthesis) [44]	Growth related protein (*yabQ)*	CYT	No interaction partner	*djlA* ← Co-chaperone protein; ***yabP*** →; *yabQ* → Growth related protein	Putative Undecaprenyl pyrophosphate phosphatase (cell wall biosynthesis) [45]	Type III secretion system (bacterial pathogenecity) [46]	Cell wall biosynthesis
2. yagM	Cell adhesion	LB, 37°C; 20 µg/ml Bicyclomycin (produces ROS, blocks cell division) [47]	Transcriptional regulator (fimZ) (involved in fimbriae production) [48]	CYT	DNA-binding protein (YagL)	*yagL* ← resolvase like prophage; ***yagM*** ←; *ykgV* ← Growth related protein	Unknown function	Unknown function	Cell adhesion under antibiotic stress
3. yagK	Glycine betaine bio-synthesis from choline (osmoprotectant) [49]	Na-Phosphate buffer, 37°C; *ΔthiI* (*thiI* is responsive to UV) [50]	Putative fimbrial usher protein (*yhcD)*	NUC	Putative ligase (GtrS)	*yagJ* → Response to X-radiation; ***yagK*** ←; *yagL* ← resolvase like prophage	CP4-57 prophage protein (cell growth/biofilm formation/ motility/ transport) [51]	Unknown function	Protection against radiation-induced stress

4. yahE	Not co-regulated	M9, 37°C; 0.3 M NaCl + 0.6% n-butanol (cause cellular stress) [52]	Putative acyl-CoA synthetase (*yahF)* (energy metabolism)	CYT	Putative NAD(P)-binding succinyl-CoA synthase (SucD) (energy metabolism)	*yahD* → Response to UV	***yahE*** →	*yahF* → Putative acyl-CoA synthetase	Unknown function	Unknown function	Energy metabolism under cellular stress
5. yahL	Cell adhesion	LB, 37°C	Membrane protein (*yahC)*	NUC	Unknown function (YahE)	*yahK* → Aldehyde reductase (involved in biofilm formation) [53]	***yahL*** →	*xtpA* → Putative transcr. regulator	Unknown function	Unknown function	Cell adhesion
6. yahM	Glycine betaine bio-synthesis from choline (osmoprotection) [49]	M9, 37°C; 25 µg/ml Kanamycin	Putative amino acid exporter (*yahN)* (Efllux of toxic sunstances) [54]	CYT	Putative replicase (YidX)	*xtpA* → Putative transcr. regulator (confers antibiotic resistance) [55]	***yahM*** →	*yahN* ← Putative amino acid exporter	Unknown function	Unknown function	Protection against stress
7. ybaA	Co-regulated (unknown regulator or function)	LB, 37°C	Putative oxido-reductase (*yohF)*	CYT	Double strand break repair protein (YegP)	*ffs* → Signal recognition particle	***ybaA*** →	*pdeB* ← Cyclic di-GMP phospho-diesterase	RNA signal recognition protein [56]	Unknown function	Oxidoreduction/ DNA damage repair
8. ybaP	Co-regulated (unknown regulator or function)	LB, 37°C	DNA binding transcriptional activator (*AaeR)* (role in biofilm formation) [57]	CYT	Cysteine-tRNA deacylase (YbaK)	*chiX* → Small regulatory RNA (role in biofilm formation) [58]	***ybaP*** ←	*ybaQ* → DNA binding transcr. regulator (regulates biofilm based response) [59]	Conjugal transfer protein	Unknown function	Biofilm formation
9. ybdJ	Not co-regulated	LB, 37°C	Putative transporter (*yeeA)* (aromatic acid exporter) [60]	PM	DUF419 family protein (YbdF)	*ybdF* ← Defense mechanism	***ybdJ*** ←	*ybdK* ← Amino acid bio-synthesis	Unknown function	Unknown function	Stress response

10. ybeR	Not co-regulated	M9, 37°C; 0.3 M NaCl + 0.6% n-butanol (cause cellular stress) [52]	Putative oxamate carbomyl-transferase (*fdrA)*	CYT	Putative co-chaperone (DjlB) (heat stress response)	*ybeQ* ← Oxidative stress response	***ybeR*** →	*djlB* → J-domain type protein	Unknown function	Unknown function	Multi-stress response
11. yceQ	Cell death	LB, 37°C	DNA binding transcriptional repressor (*acrR)* – involved in efflux of toxic substances [61]	CYT	Endoribonuclease (RNE) – adaptation to different growth conditions [62]	*Rne* ← Ribosomal nuclease	***yceQ*** →	*rluC* → 23S rRNA pseudo-uridine synthase	Unknown function	Unknown function	Cell death prevention
12. ycgX	Not co-regulated	LB, no O_2, 37°C	Membrane protein (*yigF*)	CYT	Repressor of blue light-responsive genes (BluR)	*ymgL* ← Consti-tutively expressed protein in rich medium	***ycgX*** ←	*bluR* ← DNA binding transcr. regulator	Prophage protein	Unknown function	Unclear
13. ycgY	Stress response in stationary phase	LB, no O_2, 37°C	Outer membrane protein (*yaiO)*	CYT	Uncharacterized protein (YncH)	*ymgE* → DNA Recomb-ination	***ycgY*** →	*treA* ← Trehalase protein (nutrient stress in stationary phase) [63]	Unknown function	Unknown function	Growth-associated response during stationary phase
14. ychS	Not co-regulated	LB, 37°C; 1 ug/mL of Ciprofloxacin+ 500 µM of ET2DA (cause oxidative/ cellular stress) [64]	Putative amino acid de-hydrogenase (*ykfG)* – role in oxidative stress [65]	CYT	Not found	*narI* → Nitrate reductase (oxido-reductase activity) (UniProt)	***ychS*** →	*tpr* ← Protamine like protein	Beta-galactosidase	Protein YchS (Unknown function)	Oxidative stress response

15. yciX	Not co-regulated	M9, 37°C; *yqjD* over-expression (inhibits cell growth) [66]	Membrane-associated regulatory protein (*ymiA)* (in exponential or tationary phase) [67]	CYT	Membrane-associated regulatory protein (YmiA)	*ymiA* → Membrane-associated regulatory protein	***yciX*** →	*ymiC* → Stationary phase adaptation protein	Unknown function	Unknown function	Growth-associated response during stationary phase
16. ydaF	Fucose metabolism/DNA damage response (Fucose metabolism is disrupted by prophage) [68]	LB, no O_2, 37°C	Prophage protein (*ydaG)*	CYT	Prophage protein (YdaG)	*sieB* → Phage infection exclusion protein	***ydaF*** ←	*ydaG* ← Prophage protein	Prophage protein	Unknown function	Prophage protein involved in disruption of fucose metabolism
17. ydcD	Phenylacetate catabolic process (prevalant under anaerobic conditions) [69]	LB, no O_2, 37°C	Cytoplasmic trehalase (*treF)* (osmotic stress) [70]	CYT	Putative peri-plasmic protein (YjbT)	*yncH* →	***ydcD*** →	*yncO* ← growth-related protein expressed in rich medium)	dCTP de-aminase	Unknown function	Anaerobic respiration
18. ydcH	Phenyl acetate catabolic process (prevalant under anaerobic conditions) [71]	LB, no O_2, 37°C	Transcription (*ygeV)*	CYT	Putative structural protein (YaeH)	*opgD* → Glucans synhesis protein	***ydcH*** →	*rimL* → Ribosomal transferase	Unknown function	Unknown function	Anaerobic respiration
19. ydfA	Not co-regulated	LB, no O_2, 37°C	Putative transcriptional regulator (*ygeV)*	CYT	Qin prophage (constitutively expressed, unknown function) (YdfB)	*dicA* → DNA binding transcr. regulator	***ydfA*** →	*ydfB* → Consti-tutively expressed protein	Phage protein	Unknown function	Unclear
20. ydfC	Not co-regulated	M9, 37°C; 0.3 M NaCl, + 0.6% n-butanol (causes osmotic stress) [52]	Putative carbamate kinase (*ycbF)* (biofilm formation) [72]	CYT	Qin prophage (constitutively expressed, unknown function) (YdfB)	*ydfB* → Consti-tutively expressed protein	***ydfC*** →	*dicB* → Cell division inhibition protein	Putative phage protein	Unknown function	Cellular stress response

21. ydfX	Not co-regulated	LB, 37°C	Putative glycosyl-transferase (*yefI)*	CYT	Qin prophage (transcriptional regulator) (DicA)	*ydfW* ← Response to antibiotics	***ydfX*** ←	*dicC* ← DNA-binding transcr. regulator	Bacterial toxin protein	Unknown function	Unclear
22. ydgH	Oxidoreduction (Respiratory complex I) (NADH: ubiquinone oxidoreductase, oxidative stress protection) [73]	LB, 37°C; 1ug/ml of Ciprofloxacin (FC=0.38, relative to *frr* gene)	Beta-glucosidase (*bglA)* (Bgl operon confers fitness advantage under stress) [74]	ECS	Dihydro-monapterin reductase (FolM) (role in oxidative stress) [75]	*pntA* ← Pyrimidine nucleotide hydro-genase – role in oxidative stress [76]	***ydgH*** →	*ydgI* → Putative Arginine: ornithine antiporter	YdgH/BhsA/McbA-like domain-containing protein (involved in stress response/biofilm formation and patho-genesis)	Unknown function	Oxidative stress response
23. ydiH	Co-regulated (Unknown/ regulator or function)	M9, 37°C; 10% n-hexane (oxidative stress) [77]	Cyclopropane fatty acyl phospholipid synthase (*cfa)*	CYT	Putative ferrodoxin-like lipoprotein (YdjY) (oxidative stress response) [78]	*menI* ← Mena-quinone bio-synthesis	***ydiH*** ←	*ydiK* → Putative trans-porter	Unknown function	Unknown function	Oxidative stress response
24. ydjO	Response to acidic pH (upregulation of oxidative stress response genes) [79]	MOPS, 37°C; 0.4% Glycerol + 0.5% 2-Deoxy-D-glucose	Cysteine/ selenocysteine cation transporter (*tcyP)* [80]	CYT	Cell division modulator (CedA) (induced in oxidative stress)	*tcyP* → Cation transporter	***ydjO*** ←	*cedA* ← Cell division modulator	Unknown function	Unknown function	Oxidoreduction under acidic pH conditions
25. yeaC	Aerobic respiration	LB, 37°C	Methionine sulphoxide reductase (*msrB)* (oxidative stress) response [81]	CYT	Methionine sulfoxide reductase B (MsrB)	*ydjL* ← Putative Zn-binding dehydro-genase (oxidative stress response) (UniProt)	***yeaC*** ←	*msrB* ← Meth-ionine sulphoxide reductase	Transcriptional regulator	Unknown function	Oxidative stress response during aerobic conditions

26. yebO	Cellular response to Magnesium ion (during aerobic respiration) [82]	M9, 37°C; double mutant for genes involved in aerobic respiration *(Δndh ΔcyoB)* [83]	PhoQ kinase inhibitor (*mgrB)*	PM	PhoP/PhoQ signaling protein (MgrB) (induced by low $Mg2^{+}$) [84]	*yobF* ← General stress response protein	***yebO*** ←	*mgrB* ← Kinase inhibitor	Unknown function	Unknown function	Response to magnesium ions during aerobic respiration.
27. yebW	Not co-regulated	LB, 37°C	Phospho-protein phosphatase (*pphA)*	CYT	Lipopolysaccharide biosynthesis protein (WbbK)	*yebV* → Protein binding	***yebW*** ←	*pphA* → Phospho-protein phos-phatase	Lipoprotein	DUF1482 family protein	Unclear
28. yecH	Anaerobic respiration	M9, 37°C; triple mutant of genes involved in aerobic respiration *(ΔndH, ΔcydB, ΔappC)* [83]	DNA gyrase inhibitor (*sbmC)* (involved in SOS response) [85]	CYT	Putative nucleoside tri-phosphatase (SgcQ)	*ftnA* → Ferritin iron storage protein (oxidative stress response) [86]	***yecH*** ←	*tyrP* → Tyrosine symporter	Metal-binding protein	YecH family protein	Switching from aerobic to anaerobic respiration under stress
29. yecT	Not co-regulated	M9, 37°C; 0.3 M NaCl + 0.6% n-butanol (causes osmotic stress) [52]	Multidrug/cho-line/betaine efflux transporter (*emrE)* (osmotic stress response) [87]	CYT	Putative DNA-binding transcriptional regulator (YhfZ)	*yecV* ← Expo-nential phas protein (in rich medium)	***yecT*** →	*flhE* ← Flagellar protein	Lysozyme inhibitor	LprI domain-containing protein (lipo-protein)	Osmotic stress response
30. yegJ	Cellulose biosynthetic process	LB, no O_2, 37°C	Reactive chlorine species responsive protein (*rclC)*	ECS	Putative non-specific DNA-binding protein (YegI)	*yegI* ← Ser/Thr Phos-phatase	***yegJ*** →	*pphC* ← Ser/Thr Phosp-hatase	Unknown function	Unknown function	Unclear
31. yegL	Not co-regulated	LB, no O_2, 37°C	Zinc-finger domain protein (*yehQ)*	CYT	Ser/thr phosphatase realted protein (YegK)	*pphC* ← Ser/Thr phos-phatase	***yegL*** ←	*yegR* →	Homeostasis protein	Mediator of transcription	Unclear
32. yegR	Phosphorelay signal transduction system / Oxalate catabolic	M9, 37°C; double mutant for genes involved in aerobic respiration *(Δndh ΔcyoB)* [83]	Putative oxido-reductase (*ydeP)*	ECS	Orphan protein (OrgK)	*ogrK* ← Trans-cription regulation	***yegR*** ←	*yegS* → Lipid kinase	Lipoprotein	Unknown function	Oxidoreduction

	process (involved in acid stress resistance) [88]								
33. yehI	Not co-regulated	LB, no O_2, 37°C	ATP-binding lipopolysaccharide transport protein (*msbA)*	CYT	Putative ATPase (YehL)	*yehF* → Molybdate transport regulator; ***yehI*** →; *yehK* →	Putative regulator	DUF4132 domain-containing protein	Transport protein
34. yehK	Not co-regulated	MOPS, 37°C; 0.4% Glycerol + 0.5% 2-Deoxy-D-glucose	Putative fimbrial adhesin protein (*sfmH)*	CYT	Putative ATPase (YehL)	*yehI* →; ***yehk*** →; *orzP* → Small RNA	Unknown function	Unknown function	Unclear
35. yeiS	Not co-regulated	LB, 37°C	Vanomycin responsive protein (*sanA)*	CYT	Cell membrane barrier (SanA)	*sanA* → Response to Vanomycin; ***yeiS*** →; *preT* → dehydro-genase	Vancomycin high temperature exclusion protein	Unknown function	Maintaining cell membrane integrity against drugs (e.g. Vanomycin)
36. yfbM	Aerobic respiration	M9, no O_2, 37°C	Hemolysin E (*hlyE)* (pore forming protein) [89]	CYT	Unknown function (YfbN)	*yfbL* → Putative peptidase (proteo-lysis) (EcoCyc); ***yfbM*** →; *yfbN* ←	Unknown function	DUF1877 family protein	Protein lysis
37. yfbN	Response to acidic pH	MOPS, 37°C; 0.4% Glycerol + 0.5% 2-Deoxy-D-glucose	DNA binding transcriptioal regulator (*ydeO)*	CYT	Unknown function, YfbO	*yfbM* →; ***yfbN*** ←; *yfbO* →	Unknown function	Unknown function	Unclear
38. yfbO	Not co-regulated	MOPS, 37°C; 0.4% Glycerol + 0.5% 2-Deoxy-D-glucose	Function unknown (*yfbP)*	ECS	Unknown function (YfbP)	*yfbN* ←; ***yfbO*** →; *yfbP* →	Immunity protein (cyto-toxicity)	Unknown function	Unclear
39. yfbP	Not co-regulated	M9, 37°C; 0.3 M NaCl + 0.6% n-butanol	Inner membrane protein (*ynjI)*	CYT	Putative amino-peptidase (YfbL) (Proteolysis) (EcoCyc)	*yfbO* ←; ***yfbP*** →; *nuoN* ← Oxido-reductase	Protein folding and transport	Unknown function	Protein quality control under stress
40. yfdN	Not co-regulated	LB, no O_2, 37°C	Oxidative stress response protein (*yfdO)*	CYT	Prophage protein (phage-related function) (YfdT)	*yfdM* ← Putative methyl-transferase; ***yfdN*** ←; *yfdO* ← Oxidative stress response	Transcriptional activator family protein	Unknown function	Oxidative stress response

41. yfdP	Not co-regulated	LB, no O_2, 37°C	Putative auto-transporter adhesin (*ycgV)*	CYT	Prophage protein (response to oxidative stress) (YfdS)	*yfdO* ← Oxidative stress response	***yfdP*** →	*yfdQ* → Phage-related function	Prophage protein	Unknown function	Oxidative stress response
42. yfeS	Cellular response to envelope stress	MOPS, 37°C	Putative lipoprotein (*yidX)*	CYT	Putative efflux protein (YdhK)	*yfeK* → Transcr. regulation	***yfeS*** →	*cysM* ← Cysteine synthase	Molybdate metabolism protein	Unknown function	Envelope stress response
43. yffL	Response to Nitrate/ Nitrite (anaerobic respiration)	M9, 37°C	Anaerobic glycerol-3-phosphate dehydro-genase *(glpB)* [89]	CYT	Prophage protein (Integrase) (IntZ)	*intZ* → Putative integrase	***yffL*** →	*yffM* →	Prophage protein	CPZ-55 prophage (involved in general stress response) [90]	Anaerobic respiration
44. yffM	Not co-regulated	LB, no O_2, 37°C	Alpha-mannosidase (*mngB)*	CYT	Prophage (unknown function) (YffN)	*yffL* →	***yffM*** →	*yffN* →	Unknown function	Unknown function	Unclear
45. yffN	Not co-regulated	MOPS, 37°C; 0.4% Glycerol + 0.5% 2-Deoxy-D-glucose	Tail fiber protein (*stfR)*	CYT	Prophage (unknown function) (YffM)	*yffM* →	***yffN*** →	*yffO* →	Unknown function	Unknown function	Unclear
46. yffP	Not co-regulated	M9, 37°C; 0.3 M NaCl + 0.6% n-butanol	Function unknown (*yffO)*	CYT	Prophage (unknown function) (YffO)	*yffO* →	***yffP*** →	*yffQ* →	Unknown function	Unknown function	Unclear
47. yffQ	Not co-regulated	MOPS, 37°C; 0.4% Glycerol	CRISPR-associated endo-ribonuclease (*cas2)* (defense response to virus) (EcoCyc)	CYT	Prophage (unknown function) (YffP)	*yffP* →	***yffQ*** →	*yffR* ←	Unknown function	CPZ-55 prophage (involved in general stress response) [90]	Stress response
48. yffR	Not co-regulated	M9, 37°C; triple mutant of genes involved in aerobic respiration *(ΔndH, ΔcydB, ΔappC)* [83]	Bacterial adhesion/ biofilm formation (*yhjY*)	CYT	Prophage (unknown function) (YffQ)	*yffQ* →	***yffR*** →	*yffS* → DNA bindin	Unknown function	Unknown function	Stress response

49. yfiM	Cell death	LB, 37°C	Alpha-ketoglutarate: H^+ symporter (*kgtP) (*efflux transporter for sugar-phosphate stress) [91]	ECS	Phospholipid biosynthesis protein (PssA)	*pssA* → Phos-phatidyl-serine synthase	***yfiM*** →	*kgtP* ← H^+ symporter	Lipoprotein	Unknown function	Lipoprotein with a role in mitigating the effects of cellular stress
50. yfjH	Not co-regulated	MOPS, 37°C; 0.4% Glycerol + 0.5% 2-Deoxy-D-glucose	Growth related protei (*htrL)*	CYT	Prophage (transcriptional activation) (AlpA)	*intA* → Integrase protein	***yfjH*** ←	*alpA* → Transcr. regulator	Unknown function	Unknown function	Unclear
51. yfjJ	Response to acidic pH (upregulation of genes involved in cell adhesion) [92]	MOPS, 37°C; 0.4% Glycerol and 0.5% 2-Deoxy-D-glucose	Putative fimbrial usher protein (*htrE)* – cell adhesion or pilus assembly protein [92]	CYT	Prophage (cytosolic protein) (YfjI)	*yfjI* → Prophage protein	***yfjJ*** →	*abpB* ← Putative helicase	Inovirus-type Gp2 protein (viral DNA replication)	Unknown function	Cell adhesion
52. ygdT	Not co-regulated	LB, no O_2, 37°C	Putative lipoprotein (*yidX)*	CYT	Not found	*rppH* ← RNA phospho-hydrolase	***ygdT*** ←	*mutH* → DNA repair protein	Transposase protein	Unknown function	Unclear
53. yhaL	Not co-regulated	LB, 37°C; *Δhns* (stress adaptation)	DNA binding transcriptional activator (*fucR)*	CYT	Ser/thr phosphatase-related protein (Yegk)	*yhaK* → bicupin related protein (acid stress/oxidative stress response) [93]	***yhaL*** →	*cyuA* ← L-cysteine di-sulphidase	Cytoplasmic protein	Unknown function	Stress response

54. yhdN	Response to heat	LB, 30°C (stationary phase)	DNA binding transcriptional activator (*zntR)* (stress responsive transcription factor) [94]	CYT	Transcriptional activator (ZntR)	*zntR* ← DNA binding transcr. regulator	***yhdN*** ←	*rplQ* ← 50S ribosome subunit protein (protein bio-genesis) [95]	Conserved protein	DUF1992 domain-containing protein (conserved protein belonging to the DNAJ homolog family, heat shock response) (UniProt)	Regulation of heat shock response, expressed during stationary phase
55. yhfU	Not co-regulated	M9, 37°C; 0.3 M NaCl + 0.6% n-butanol (osmotic stress) [53]	Aromatic carboxylic acid efflux pump (*aaeA)* (involved in defense mechanisms) [96]	CYT	Putative transport protein (YhfT)	*yhfT* ← Membrane protein	***yhfU*** ←	*php* ← Putative hydrolase	Unknown function	Unknown function	Osmotic stress response
56. yhhL	Not co-regulated	LB, 37°C; *ΔdsrA* (gene involved in stress response, biofilm formation) [97]	16S rRNA methyl-transferase (*rsmD)*	CYT	16S rRNA methyl-Transferase (RsmD)	*rsmD* → 16S rRNA methyl transferase	***yhhL*** → xs	*yhhM* ← Quorum sensing protein – (stress response, biofilm formation) [98]	rRNA small subunit methyl-transferase protein	Unknown function	Biofilm formation
57. yibI	Response to nitrosative stress (redox stress) [99]	M9, 37°C; 0.3 M NaCl + 0.6% n-butanol (osmotic stress) [52]	Inner membrane protein (*yibH)* (stress response) [100]	PM	Inner membrane protein (YibH)	*yibH* ← Inner membrane protein	***yibI*** ←	*mtlA* → mannitol-specific PTS enzyme	Inner membrane protein	Unknown function	Stress response protein.
58. yicN	Not co-regulated	LB, 37°C; *Δhns* (stress adaptation) [101]	DNA binding transcriptional regulator (*frlR)*	CYT	Putative Transporter (NepI)	*nepI* ← Purine ribo-nucleoside exporter	***yicN*** ←	*adeQ* ← Adenine trans-porter	Unknown function	Unknown function	Nucleotide transport

59. yidB	Not co-regulated	LB, 37°C; triple mutant of genes involved in respiration *(ΔndH, ΔcydB, ΔappC)* [83]	Bitopic inner membrane protein (*ypfJ)*	CYT	Sugar phosphate phosphatas (YidA) (phosphate metabolism) [102]	*yidA* ← Sugar phos-phatase	***yidB*** ←	*gyrB* ← DNA gyrase	Radical SAM domain-containing protein	Unknown function	Unclear
60. yigA	Not co-regulated	LB, 37°C	Diamino-pimelate epimerase (*dapF)* (cell wall biosynthesis) [103]	CYT	Diamino-pimelate epimerase (DapF) (cell wall structure) [104]	*dapF* → diamino-pimelate epimerase	***yigA*** →	*xerC* → Tyrosine recombi-nase	Diamino-pimelate epimerase protein	Not found	Cell wall biosynthesis
61. yigE	Not coregulated	LB, no O_2, 37°C	Putative magnesium chelatase (*yifB)* (chaperonic activity) [105]	CYT	Inner membrane protein (YedI)	*uvrD* → DNA helicase	***yigE*** ←	*ysgD* → Consti-tutively expressed protein (in rich medium)	Phospho-diester glycosidase family protein	Anaerobic nucleoside-tri-phosphate reductase-activating protein (DNA synthesis and repair) [106]	Stress response during anaerobic conditions
62. yjbD	Not coregulated	M9, 37°C; 10% n-hexane	Putative methyl-transferase (*yafS)*	CYT	Cysteine cluster protein (YcgN)	*rluF* → Pseudo-uridine synthase	***yjbD*** ←	*lysC* ← Aspartate kinase	Unknown function	Unknown function	Unclear
63. yjbL	Response to acidic pH	LB, no O_2, 37°C	Cell envelope stress response protein (*yqcG)*	CYT	Uncharacterized protein (YjbM)	*zur* ← Transcr. regulator	***yjbL*** →	*yjbM* → Cell-envelope related protein	Unknown function	Unknown function	Envelope stress response under stress
64. yjbS	Response to acidic pH (upregulation of oxidative stress response genes) [107]	M9, 37°C; 10µg/ml Mitomycin-C (genotoxic agent, ROS producing) [108]	Pathogenicity-related (*yqeK)*	CYT	Putative oxido-Reductase (YqiJ) ([109]	*tyrB* → Tyrosine amino-transferase	***yjbS*** ←	*aphA* → Acid phos-phatase	Unknown function	Unknown function	Oxidative stress response.
65. yjcB	Carbohydrate transport	M9, no phosphate, 37°C; *ΔphoB* (phosphate transport gene)	Capsule synthesis regulator (*rcsB)*	CYT	Putative peri-plasmic protein (YpeC)	*ssb* → ss-DNA binding protein	***yjcB*** ←	*pdeC* → Cyclic di-GMP Phospho-diesterase	Membrane protein	Not found	Unclear

66. yjcF	Response to acidic pH	LB, 37°C	Pathogenicity-related (*ygeH)*	CYT	Ribosomal silencing factor (RsfS)	*yjcE* → Putative transporter	***yjcF*** ←	*actP* ← Cation trans-porter	Unknown function	Unknown function	Unclear
67. yjdI	Oxidoreduction (Respiratory complex I)	LB, 37°C; triple mutant of genes involved in respiration *(ΔndH, ΔcydB, ΔappC)*	Putative N-acetyl-Transferase (*yjdJ)*	CYT	Putative N-acetyl-Transferase (YjdJ)	*dcuS* ← Sensor histidine kinase	***yjdI*** →	*yjdJ* → Putative acetyl-trans-ferase	Unknown function	Fer4_19 domain-containing protein (involved in iron-sulphur binding)	Aerobic respiration
68. yjeJ	Cell adhesion	LB, 37°C; HS, 50°C for 7'	6-phospho-gluconate phosphatase (*yieH)*	CYT	Lysylation protein (EpmB)	*yejI* → Lipoprotein (heat shock response) [110]	***yjeJ*** ←	*epmB* ← Lysine amino-mutase	Unknown function	Unknown function	Cell adhesion under heat shock response
69. yjeT	Not coregulated	LB, 37°C; HS, 50°C for 15'	Lipo-polysaccharid e core heptose kinase *(waaP)*	CYT	HflB protease modulator (HflC) (in heat shock response) [111]	*hflC* → ftsH protease regulator (heat shock response) [111]	***yjeT*** →	*purA* → Adenylo-suucinate syn-thetase	Unknown function	Unknown function	Heat shock response
70. yjfI	Coregulated (unknown regulator or function)	LB, 37°C, reaction buffer (with Lysine)	Inner membrane protein (*yjgN)*	CYT	Membrane chaperone family protein (YjfJ) [112]	*rlmB* → Methyl-transferase	***yjfI*** →	*yjfJ* → Transcr. regulator	Cytoplasmic protein	Unknown function	Unclear
71. yjfK	Not coregulated	LB, no O_2, 37°C	Membrane chaperone family protein (*yjfJ)*	CYT	Inner membrane protein (YjfL)	*yjfJ* → Transcr. regulator	***yjfK*** →	*yjfL* → Inner membrane protein	Unknown function	Unknown function	Unclear
72. yjfZ	Not coregulated	LB, 37°C	Acyl transferase (*yihG)*	CYT	Putative inner membrane poly-saccharide flippase (YghQ)	*rpiI* → Ribosomal subunit protein	***yjfZ*** ←	*ytfB* ← Cell division	Unknown function	Unknown function	Unclear

73. yjgR	Not coregulated	LB, no O_2, 37°C	NADPH dependent aldehyde reductase (*ahR)*	PM	L-idonate and D-gluconate transporter (IdnT)	*iptG* → LPS Transport system	***yjgR*** ←	*idnR* ← DNA binding transcr. regulator	Ornithine amino-transferase	Conjugal transfer protein	Transport
74. yjgZ	Coregulated (unknown regulator or function)	M9, 37°C; 0.3 M NaCl + 0.6% n-butanol	Putative multidrug efflux pump (*mdtO)*	CYT	Putative receptor protein (YhhM)	*insD6* → Trans-posase	***yjgZ*** →	*insG* ← Putative transposase	Transposase	Unknown function	Unclear
75. yjjY	Cell death	LB, 37°C	DNA binding transcriptional regulator (*arcA)*	CYT	Uncharacterized protein YniD	*arcA* ← DNA binding transcr. regulator	***yjjY*** →	*ytjE* → Growth related protein	Unknown function	Unknown function	Unclear
76. ykgL	Glycine betaine biosynthesis from choline [49]	M9, 37°C; *ΔkdpE*; Tris-maleic acid+115 mM KCl (disrupts potassium uptake under osmotic stress) [113]	50S ribosomal subunit protein (*ykgM)*	CYT	Carnitinyl-CoA dehydratase (CaiD) – osmoprotectant protein [114]	*matA* ← DNA binding transcr. regulator	***ykgL*** →	*ykgO* ← 50S ribosomal subunit protein	Unknown function	Unknown function	Osmotic stress response.
77. ylcH	Trans-criptional attenuation	M9, 37°C; 0.3 M NaCl + 0.6% n-butanol	Ionic detergents response protein (*yfbK)*	No inf.	Uncharacterized protein (YlcG)	*ybcM* → DNA binding transcr. regulator	***ylcH*** →	*ybcN* → DNA base-flipping protein	Unknown function	Unknown function	Unclear
78. ylcI	Aerobic respiration	LB, 37°C; double mutant of genes involved in respiration *(ΔndH, ΔcyoB)*	Phage related protein (*ybcW)*	CYT	Oxidoreductase (NuoM) – involved in aerobic respiration [115]	*ybcW* → Prophage protein	***ylcI*** ←	*nohD* → DNA packing protein	Unknown function	DUF3950 domain-containing protein	Aerobic respiration
79. ymfI	DNA restriction/ modification system	LB, 37°C; 1 ug/mL of Ciprofloxacin+ 500 µM of ET2DA	Phage related protein (*ymfJ)*	CYT	Uncharacterized protein (*ymfJ)*	*ymfH* ← Prophage protein	***ymfI*** →	*ymfJ* ← Prophage protein	Phage protein	Unknown function	Unclear
80. ymgI	Not co-regulated	M9, no phosphate, 37°C; *ΔphoB* (phosphate transport gene)	Heat shock responsive protein (ymgG)	CYT	Cell division topological specificity protein (MinE)	*ymgG* ← Heat shock response protein	***ymgI*** ←	*ymgJ* →	Unknown function	Unknown function	Unclear

81. ymgJ	Not co-regulated	M9, 37°C; 0.3 M NaCl + 0.6% n-butanol	Putative fimbrial usher protein (*htrE)* (heat shock response) [116]	CYT	Heat shock response protein (YmgG)	*ymgI* ←	***ymgJ*** →	*minE* ← Cell division	Transposase protein	Unknown function	Heat shock response
82. ynaJ	Aerobic respiration	LB, 37°C	ADP-sugar diphosphatase (*nudE)*	CYT	Translation-realted protein (YciU)	*insH4* → Trans-posase	***ynaJ*** →	*uspE* ← Universal stress protein	Inner membrane protein	Unknown function	Unclear
83. yncH	Response to acidic pH	LB, 37°C; *rpoD* overexpression (response to heat) [117]	Cell envelope stress response protein (yqcG)	CYT	Glutathione S-transferase homolog (YncG)	*yncG* → Putative Glutata-thione-S transferase	***yncH*** →	*yncO* ← Consti-tutively expressed protein (in rich medium)	Unknown function	Unknown function	Stress response
84. yneG	Not co-regulated	M9, no ammonium, 37°C	Glutaminase (*glsB)* Ammonium assimilation [118]	CYT	Putative Glutaminase (GlsB) (amino acid metabolism) [119]	*dgcF* ← Putative Di-guanylate cyclase	***yneG*** ←	*glsB* ← Glutaminase	Cytoplasmic protein	Unknown function	Nitrogen metabolism during ammonium limitation
85. yneK	Not co-regulated	MOPS, 37°C; 0.4% Glycerol + 0.5% 2-Deoxy-D-glucose (metabolic stress) [120]	Putative fimbrial usher protein (*htrE)* (heat shock response) [116]	CYT	Putative oxido-reductase (YdhF)	*ptrR* → L-glutamate meta-bolism	***yneK*** →	*ydeA* → L-arabinose exporter	Unknown function	Unknown function	Stress response
86. ynfO	Anaerobic respiration	LB, 37°C; 100 µg/ml Ampicillin	Function unknown (*ylcI)*	CYT	Putative (D)-galactarate transporter (GarP)	*nohA* ← Prophage protein	***ynfO*** →	*ydfO* → Prophage protein	Unknown function	DUF3950 domain-containing protein	Unclear
87. yoaC	Not co-regulated	LB, 37°C	Lipoprotein (*yfiL)*	CYT	Protein export (MsyB)	*yoaB* → Biofilm based activity	***yoaC*** →	*yoaH* ←	Unknown function	Unknown function	Unclear

88. yoaH	Not co-regulated	LB, 37°C; *Δhns* (stress adaptation)	DNA-binding transcriptional repressor *(acrR)*	CYT	DUF1889 family protein (YoaC)	*yoaC* →	***yoaH*** ←	*pabB* → Amino-deoxy-choris-mate synthase	Unknown function	Unknown function	Unclear
89. yodC	Oxidoreduction (Respiratory complex I)	LB, 37°C	Putative adenosine mono-phosphate *(fic)*	CYT	Ribosome modulation protein (RmF) (response to oxidative stress) [121]	*dgcQ* ← Di-guanylate cyclase	***yodC*** ←	*yedI* ← Inner mem-brane protein	Cytoplasmic protein	Unknown function	Oxidoreduction
90. ypaB	Not coregulated	M9, 37°C; 0.3 M NaCl +0.6% n-butanol	Putative fimbrial chaperone *(yadV)*	CYT	Not found	*yfaL* ← Putative auto-transporter adhesin	***ypaB*** ←	*nrdA* → Ribo-nucleoside reductase	Transposase	Unknown function	Unclear
91. ypeB	Ribosome structure	M9, 37°C; 50 mM isoprenol	Tetraacyl-disaccharide 4'-kinase *(lpxK)*	CYT	DNA ligase (LigA)	*yfeH* → Putative Na^+ symporter	***ypeB*** ←	*ligA* ← DNA ligase	Cytoplasmic protein	Cyto-plasmic protein	Unclear
92. ypjB	Not coregulated	LB, no O_2, 37°C	Putative type III secreted effector *(yqeK)* (bacterial patho-genecity) [122]	CYT	Not found	*ypjA* ← auto-transporter	***ypjB*** ←	*ypjC* ← Patho-genicity	Uncharacteriz ed protein	Unknown function	Pathogenecity
93. yrdB	Oxidoreduction (Respiratory complex I)	LB, 37°C	Shikimate dehydro-genase *(aroE)*	CYT	Dehydro-shikimate reductase (AroE) - oxidative stress response) [123]	*yrdA* → carbonic anhydrase	***yrdB*** ←	*aroE* ← shikimate anhydrase	DUF1488 domain-containing protein	Unknown function	Oxidoreduction
94. yrhD	Response to acidic pH	LB, no O_2, 37°C	Putative type III secreted effector *(yqeK)* (bacterial patho-genecity) [122]	CYT	Not found	IS1E → Insertion sequence	***yrhD*** →	*yrhB* → Putative HS chaperone	Unknown function	Unknown function	Unclear
95. ytiA	Not co-regulated	LB, no O_2, 37°C	Putative transporter *(yjiJ)*	CYT	Not found	*yjiK* ← Membrane	***ytiA*** ←	*yjiL* ← Putative de-	DUF3343 domain-containing	Unknown function	Unclear

						protein	hydratase	protein	

Abbreviations: ATP, Adenosine triphosphate; dCTP, Deoxycytidine triphosphate; ET2DA, Ethyl trans-2-decenoic acid; HS, Heat shock; KCl, Potassium chloride; LB, Luria Bertani; LPS, Lipopolysaccharide; M9, Minimal medium; MOPS, 3-(N-morpholino) propanesulfonic acid; NADP, Nicotinamide dinucleotide phosphate; PTS, phosphotransferase system; ROS, Reactive oxygen species; SAM, S-adenosylmethionine; Ser/Thr, Serine/Threonine; Transcr. , Transcription

251 Genes with a higher confidence in the inference section (green) were analysed for candidates
252 to be used for *in vitro* testing. Three HP-encoding genes, namely *yhdN*, *yeaC*, and *ydgH*, were
253 selected for further analysis (highlighted in grey) (**Table 1).**
254
255 **Protein encoding gene *yhdN***
256 Protein YhdN, characterized by the presence of a domain of unknown function (DUF1992),
257 was predicted to be involved in heat shock response. The gene encoding *yhdN* is regulated
258 by the RNA polymerase sigma factor RpoH (σ32), which serves as the primary heat shock
259 transcriptional regulator. Under normal conditions, RpoH levels are kept low due to chaperone-
260 mediated degradation; however, these levels increase significantly upon heat shock [124].
261 Gene Ontology (GO) annotation for this cluster is categorized under 'response to heat'. Based
262 on publicly available transcriptomic data [43], the *yhdN* gene exhibited significant expression
263 in cells grown to the stationary phase, with a Log_2FC of 5.5 relative to the reference gene *frr*,
264 signifying a 45 times higher expression of *yhdN* gene. This observation suggests that
265 the *yhdN* gene is highly expressed during the stationary phase and therefore might have a
266 role in nutrient stress response. Additionally, *yhdN* expression was upregulated following
267 exposure to a transient heat shock at 50°C for 15 minutes, with a Log_2FC of 4.8 and 27 times
268 higher expression, suggesting that the gene might also play a role in heat shock response.
269 Co-expression analysis using Spearman correlation of the gene resulted in a high correlation
270 with the gene *zntR* (0.93) encoding an HTH (helix-turn-helix)-type transcriptional regulator
271 [125] which is involved in protein stability and prevention of aggregates [126,127]. Genes *yhdN*
272 and *zntR* are also part of the same transcription unit (EcoCyc database). Other genes with
273 high correlations to *yhdN* were *relB* (0.84)*, pspB* (0.84) *and pspC* (0.84), all of which are
274 involved in stress response [128] (*Supplementary Figure 3A.*). Gene *relB* encodes for an
275 antitoxin protein involved in regulation of growth [129] while genes *pspB* and *pspC* encode for
276 phage shock proteins that are known to be induced by infection with bacteriophages or
277 ethanol, osmotic and/or nutrient stress as well as heat shock conditions [130]. Protein-protein
278 interaction (PPI) analysis showed highest interaction confidence with ZntR. The local genomic

279 context analysis showed genes *zntR* and *rplQ* (a ribosomal subunit protein) as neighbouring
280 genes. Protein YhdN showed remote sequence homology to a protein cluster comprising of
281 uncharacterized conserved proteins and was structurally homologous to conserved proteins
282 with similarity to J-domains of chaperones, regulating the activity of heat-shock proteins [131].
283 To elucidate the potential function of *yhdN*, we hypothesized that its absence would affect
284 bacterial growth under heat shock conditions and possibly the cells stationary phase under
285 nutrient limitation. This hypothesis was tested by comparing the growth patterns of the
286 *E. coli* K-12 substrain BW25113 wild type and its isogenic *ΔyhdN* knockout mutant under a
287 transient heat shock condition (50°C) and recovery at 37°C in LB and nutrient-limited M9
288 medium.
289
290 **Protein encoding gene *yeaC***
291 Protein YeaC is characterized by the presence of a DUF1315 domain. Gene *yeaC* is predicted
292 to be governed by the regulator ArcA, which regulates a group of proteins involved in redox
293 homeostasis and aerobic respiration [132]. The Gene Ontology (GO) annotation for this cluster
294 was predicted as 'aerobic respiration'. Analysis of gene *yeaC* in publicly available
295 transcriptomic datasets showed slightly higher expression levels against gene *frr* in LB
296 medium at 37°C under normal O_2 conditions ($\log_2$ FC 1.9) (**Table1**) and in knock-out mutants
297 for genes encoding type II NADH:quinone oxidoreductase (*ndh*), Cytochrome bd-I ubiquinol
298 oxidase (*cydB*) and Cytochrome bd-II ubiquinol oxidase (*appC*), involved in the Tricarboxylic
299 acid cycle or oxidative phosphorylation [133] ($\log_2$ FC 1.7). Based on the co-expression
300 analysis of public data, the highest correlation was observed with a gene encoding for a
301 peptide methionine sulfoxide reductase (*msrB),* which is an oxidoreductase and known to be
302 highly expressed during oxidative stress to maintain the cell-redox homeostasis [134]
303 (*Supplementary Figure3B.*). Other highly correlated genes involved succinate dehydrogenase
304 cytochrome b556 subunit (*sdhC)*, succinate dehydrogenase hydrophobic membrane anchor
305 subunit (*sdhD)* and Fumarate hydratase class I, aerobic (*fumA),* which are all involved in the
306 tricarboxylic acid or TCA cycle [135,136] (*Supplementary Figure 3B.*). PPI analysis also

307 showed highest interaction confidence with MsrB. Additionally, it neighbours the *msrB* gene
308 and a putative zinc-binding dehydrogenase, *ydjL* which is also involved in oxidoreduction
309 (UniProt) (**Table 1**). Protein YeaC shows remote sequence homology to other proteins
310 involved in transcriptional regulation. Structural homology revealed similarities to a group of
311 uncharacterized proteins with unknown functions. We hypothesized that *yeaC* affects the cell-
312 redox homeostasis and cellular growth under oxidative stress. This hypothesis was tested by
313 comparing the growth patterns of the *E. coli* K-12 substrain BW25113 wild type and its isogenic
314 *ΔyeaC* knockout mutant with a sub-lethal concentration of H_2O_2 (2.5 mM) [137].
315
316 **Protein encoding gene *ydgH***
317 Protein YdgH has a DUF1471 domain of unknown function. It is predicted to be part of an
318 unknown cluster, with no information on its regulator. The GO annotation for this cluster,
319 however, is categorized under oxidoreduction (complex I). The energy-converting
320 NADH:ubiquinone oxidoreductase respiratory complex I, is the main entry point for electrons
321 from NADH into the respiratory chains in bacteria [138]. Based on the public datasets, we
322 could not obtain a gene-specific condition where gene *ydgH* had higher expression compared
323 to gene *frr.* Co-expression analysis of *ydgH* from the publicly available RNAseq datasets
324 revealed highest correlation with a 6-phospho-beta-glucosidase (*bglA*) encoding hydrolase,
325 involved in the hydrolysis of phosphorylated beta-glucosides [139]. Other highly correlated
326 genes were phosphoglycolate phosphatase *(gph)* [140] and ribulose-phosphate 3-epimerase
327 *(rpe)* [141], involved in oxidative stress response (*Supplementary Figure 3C.*). PPI analysis
328 showed highest interaction confidence with YjfY*,* a putative HP, with a possible role in stress
329 resistance (UniProt). Genomic context provided information on a neighbouring upstream gene
330 involved in $NAD(P)^+$ transhydrogenase activity, annotated as NAD(P) transhydrogenase,
331 *pntA*, which is known to play a role in oxidative stress [142]. The protein showed remote
332 sequence homology to a YdgH/BhsA/McbA-like domain involved in stress response/biofilm
333 formation and pathogenesis [143]. The structural similarity was only to uncharacterized
334 proteins with unknown function. Following a similar hypothesis to that proposed for *yeaC*, we

335 evaluated the growth patterns of the wild type and its isogenic *ΔydgH* knockout mutant under
336 oxidative stress.
337
338 ***In vitro* analyses of candidate proteins**
339 Effect of heat shock on growth
340 To determine the effect of a transient heat shock at 50°C (7 minutes), the wild type and the
341 mutant ***Δ****yhdN E. coli* BW25113 strains were grown in LB medium. The *yhdN* mutant was seen
342 to have a growth defect of ~18% after 6h of growth based on the OD values obtained (**Figure**
343 **3A**). It was observed that after 6h of growth, the mutant could not resume normal growth
344 compared to the wild type. Additionally, the effects of a transient heat shock in Nitrogen-limited
345 M9 medium showed a significant growth defect of ~50% (**Figure 3B**). Growth curves for WT
346 and ***Δ****yhdN* in different temperatures can be found in the supplementary (*Supplementary*
347 *Figure 4A.*). Growth defects were also observed in the *yhdN* mutant compared to the wild type
348 when both the strains were grown continuously at 50°C. Since growth at 50°C is however
349 severely inhibited and cell started dying after 3h (*Supplementary Figure 4B.*), it was difficult to
350 say whether this was solely based on the absence of the protein YhdN in the mutant cells.
351
352 Effect of sublethal H_2O_2 concentration on growth
353 To determine the effect of sublethal H_2O_2 concentration, the wild type (WT), ***Δ****ydgH* and ***Δ****yeaC*
354 *E. coli* BW25113 strains were grown in LB medium until an OD of 0.2 and then exposed to an
355 H_2O_2 concentration of 2.5 mM, which is known to causes DNA damage and oxidative stress
356 [143] (**Figure 3C & D**). To study the responses due to oxidative stress, the absorbance values
357 (OD_{600}) after each hour over a 5h time period were measured. H_2O_2 was added to the cell
358 culture during the exponential phase of growth, which is characterized by rapid cell division
359 and metabolic activity and where the quorum-sensing signalling, i.e. process which allows the
360 bacteria to communicate and adjust gene expression according to cell density, is minimal.
361 Under non-stress conditions, the WT and mutant strains (*ΔydgH* and *ΔyeaC*) exhibited
362 comparable growth, with no significant differences observed. A growth lag was observed in

363 the mutants (*ΔydgH* and *ΔyeaC*) as compared to wild type when the medium was
364 supplemented with 2.5 mM H_2O_2. A growth defect of ~25% was observed in the mutant when
365 WT was compared to *ΔyeaC* at the 1h timepoint. This was reduced to ~7% after 5h of growth
366 underscoring the probability of the gene being expressed at this time point to counterfeit the
367 oxidative stress. Similarly, a growth defect of ~36% was observed in *ΔydgH* as compared to
368 WT at 1h, which decreased to ~2% after 5h, again probably due to stress adaptation and
369 expression of gene *ydgH*.
370

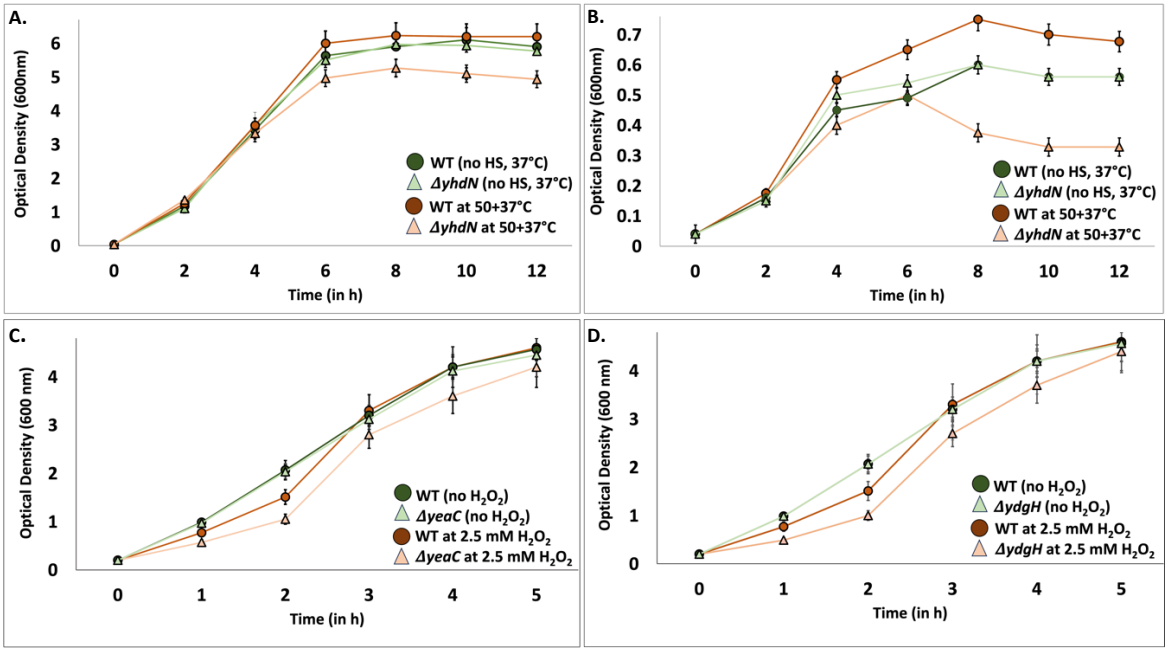

371
372
373 **Figure 3. Growth curves of *E.* coli K-12 BW25113 wild type (WT) and isogenic deletion mutants.**
374 **(A, B)** Effect of transient heat shock on WT and *ΔyhdN* cells. WT and the respective mutant strain were
375 exposed to a transient heat shock at 50°C for 7 minutes, (at OD_{600} nm = 0.04) and grown for 12 h in **A.**
376 LB medium and **B.** in Nitrogen-limited M9 medium. **(C, D)** Bacterial growth of WT and respective
377 mutants at 37°C exposed to sub-lethal concentration of 2.5 mM H_2O_2, added during the exponential
378 phase (OD_{600} = 0.2) and grown for 5h. **C.** WT and *ΔyeaC* and D. WT and *ΔydgH* cells. WT are indicated
379 by filled circles (●) and mutants by filled triangles (▲). Green lines represent controls, orange lines stress
380 conditions. Average of three independent readings taken for each specified condition. Error bars on the
381 graph indicate standard deviation from the mean.
382

383 **Differential gene expression analysis**

384 For a comparative analysis of differentially expressed genes (DEGs) and their functions in WT
385 *vs.* the mutant strains, all up- and down-regulated genes were analysed (*Figshare* > *DEGs* >
386 *Table1*). For positively regulated DEGs, representing genes upregulated in the WT strain, a

387 Log_2 fold change (Log_2FC) threshold of ≥1.5 was applied, corresponding to a minimum 2.8-
388 fold increase in expression levels. This cut-off ensured the inclusion of genes with significant
389 upregulation while minimizing noise [144]. Conversely, for negatively regulated DEGs,
390 corresponding to genes upregulated in the mutant strains, a Log2FC threshold of ≤-1.5 was
391 used.
392
393 WT *vs. ⊿yhdN*
394 Analysis of the WT strain at the 2h and 6h time points showed that *yhdN* was only significantly
395 expressed after 6h, hence this time point was chosen. In total, 484 DEGs (p_{adj}≤0.1) were
396 identified, (181) 213 genes with a positive Log_2 FC and 271 with a negative Log_2FC of 1.5.
397 Within the positive DEGs, an analysis of the top 10 genes, resulted in one gene involved in
398 protein folding, five in stress response and four in motility/chemotaxis (**Figure 4A**).
399 Significantly upregulated genes in the WT strain were *tdcB* (Log_2 FC=7.37) and *pyrB* (Log_2
400 FC=6.14). *tdcB*, encoding for threonine dehydratase is known for being expressed during
401 nutrient deprivation (EcoCyc) and gene *pyrB* is involved in pyrimidine metabolism and
402 associated with motility under stress [145]. Gene *tnaA* (Log_2 FC=6.02), which encodes for
403 tryptophanase, has been recently studied for its role in protein folding and dissolution of protein
404 aggregates [146]. Motility and chemotaxis genes such as *fliL* (Log_2 FC=6.24)*, flgD* (Log_2
405 FC=5.99) are also known to be involved in response to environmental stresses [147].
406
407 In the deletion mutant (*⊿yhdN*), the top ten negative DEGs included two genes involved in
408 heat shock, six in some type of stress response and interestingly two other were
409 uncharacterized hypothetical proteins. *bolA* (Log_2 FC=-5.53)*,* a DNA binding transcriptional
410 regulator, plays a role in cellular stress response including heat stress [148] and *mgtS* (Log_2
411 FC=-5.01), a small inner membrane protein encoding gene, is known to be expressed upon
412 heat shock [149] (**Figure 4A**). Other upregulated genes in *⊿yhdN* involved *glgS* (Log_2 FC=-
413 5.34), encoding for a surface composition regulator for biofilms and *ymgA* (Log_2 FC=-4.44)
414 encoding a putative two-component system connector protein, known to play an important role

415 in biofilm formation (EcoCyc). Upregulation of these genes in the deletion mutant suggests a
416 compensatory mechanism to mitigate stress. Additionally, a HP-encoding gene, *yodC* was
417 also upregulated (Log_2 FC=-6.39) in *ΔyhdN*. Interestingly, this gene was predicted to play a
418 role in oxidoreduction (**Table1)**. The results of this transcriptomic experiment could further aid
419 in forming a hypothesis of this gene for *in vitro* testing. Another HP-encoding gene *yffR* (Log_2
420 FC=-4.85), was predicted to play a role in stress response (this study, Table 1) which aligns
421 with the fact that a majority of stress-response genes were upregulated in the WT, when gene
422 *yhdN* is present.
423
424 All observations highlight WT strain's prioritization of growth and motility, possibly facilitating
425 better environmental sensing and resource acquisition under stress while the absence of *yhdN*
426 gene seems to upregulate other heat shock and stress response genes which reorient
427 metabolic processes towards alternative survival strategies such as biofilm formation. Hence,
428 the protein encoding gene *yhdN* is predicted to be a stress response gene involved in the
429 regulation of heat shock or nutrient limitation response, possibly also playing a broader role in
430 general stress response.
431
432 WT *vs. ΔyeaC*
433 In WT strain, the *yeaC* gene exhibited a significant upregulation after the 5h, with a log_2 FC of
434 3 relative to the 1h time point, where its expression was undetectable. This log_2FC
435 corresponds to an 8-fold increase in expression. Hence, the 5h time point was chosen for the
436 analysis. A total of 156 DEGs for WT *vs. ΔyeaC* were obtained after filtering (p_{adj}≤0.1). In WT
437 *vs. yeaC*, 87 genes had a positive Log_2 FC while 69 had a negative Log_2 FC.
438
439 Analysis of the top ten upregulated DEGs in the WT strain resulted in three oxidative stress
440 response genes, two other stress response genes, two methionine biosynthesis genes and
441 three genes involved in bacterial secretion system and transposition (EcoCyc). The
442 upregulation of the latter three genes in WT was difficult to explain, since there was no

443 conclusive literature available (**Figure 4B**). Significantly upregulated DEGs involved *ymcE*
444 (Log_2 FC=6.81) which provides tolerance to n-butanol [145], and is also known to provide
445 protection against oxidative stress [150], *prpE* (Log_2 FC=4.75) which responds to hydrogen
446 peroxide [151] and *iprA* (Log_2 FC=4.34), which encodes for an inhibitor of hydrogen peroxide
447 [152]. *metF* (Log_2 FC=4.49), a methionine biosynthesis gene, is also known to provide
448 protection against oxidative stress: Methionine is a precursor in the synthesis of cysteine,
449 which is a component of glutathione—a major intracellular antioxidant. Glutathione is known
450 to neutralize reactive oxygen species [153].
451
452 All of the upregulated genes in *ΔyeaC* were involved in motility/chemotaxis-based functions
453 (**Figure 4B**). Significantly upregulated DEGs included genes like *fliF* (Log_2 FC=-9.86), *fliO*
454 (Log_2 FC=-9.26) and *fliJ* (Log_2 FC=-9.26). The upregulation of these genes in *ΔyeaC* signify
455 that the cells prioritize the expression of motility-based genes. They are known to aid the
456 bacterium in adapting to environmental changes by modulating their expression [154].
457 Moreover, there is often a trade-off between motility and stress resistance. Studies have
458 shown that hypermotile *E. coli* strains, which exhibit increased expression of motility genes,
459 may have reduced expression of stress resistance genes, as was also observed in the
460 downregulated DEGs in the WT. Hence, as opposed to WT, the deletion mutant prioritizes
461 motility and chemotaxis to mitigate oxidative stress.
462
463 WT *vs. ΔydgH*
464 The *ydgH* gene demonstrated an upregulation after the 5h, with a log_2FC of approximately 3.7
465 as compared to 1 hour, indicating a 13-fold increase in expression. Hence, also in this case
466 the 5h time point was chosen for further analysis. A total of 231 DEGs were obtained after
467 filtering ($p_{adj} \leq 0.1$), resulting in 111 genes with a positive Log_2 FC and 120 genes with a negative
468 Log_2 FC.
469

470 Top ten positive DEGs (Log_2 FC≥1.5) involved six stress response genes, one protein
471 transport gene, one membrane biosynthesis gene, one fatty acid oxidation gene and one HP-
472 encoding gene (**Figure 4C**). Significantly upregulated genes were *dsrB* (Log_2 FC=3.89),
473 encoding for a putative stress response protein [155] and *ghoS,* (Log_2 FC=3.65), an antitoxin
474 protein which prevents cell death [156]. Gene *fadM* (Log_2 FC=2.4), encoding a thioesterase,
475 is responsible for breaking down fatty acids into acetyl-CoA units, which can then be utilized
476 in energy production [157]. Another gene, *tatE* (Log_2 FC=2.69) encoding for a transporter, is
477 involved in transport of folded proteins and maintaining of cellular redox balance [158]. Gene
478 *yoaH,* a HP-encoding gene whose function was previously unclear from **Table 1**, might also
479 play a role in oxidative stress response and should be further investigated. The role of
480 lipopolysaccharide biosynthesis gene *ais* (Log_2 FC= 2.41) was, however, unclear.
481
482 In the deletion mutant (*ΔydgH*), the top ten negative DEGs included eight motility/chemotaxis
483 genes along with one sulphur metabolism and one urate transport gene (**Figure 4C**): *fliF* (Log_2
484 FC=-6.92) and *fliA* (Log_2 FC=-5.18) play a crucial role for motility (EcoCyc), *uacT* (Log_2 FC=-
485 6.22) is involved in urate transport, which has already been studied to reduce the effects of
486 oxidative stress in *E. coli* [159]. The role of gene *cysP* regarding oxygen stress, which is
487 involved in sulphur metabolism [160] is unclear at the moment and calls for further
488 investigation.
489
490 In WT, the upregulation of genes involved in response to stress, i.e. *ghoS* suggest that the
491 cells prioritize conservation of resources by entering a dormant state, i.e. formation of persister
492 cells [156]. Due to the absence of *ΔydgH* the cell seems to attempt to compensate for the loss
493 of oxidoreductive function by utilizing genes related to motility and chemotaxis (**Figure 4C**).
494 This increased expression could be an adaptive response to maintain survival under
495 continuous exposure to oxidative stress. Hence, similar to the previous case (WT *vs. ΔyeaC*),
496 more stress response genes were upregulated in WT while motility/chemotaxis genes were
497 upregulated in *ΔydgH*.

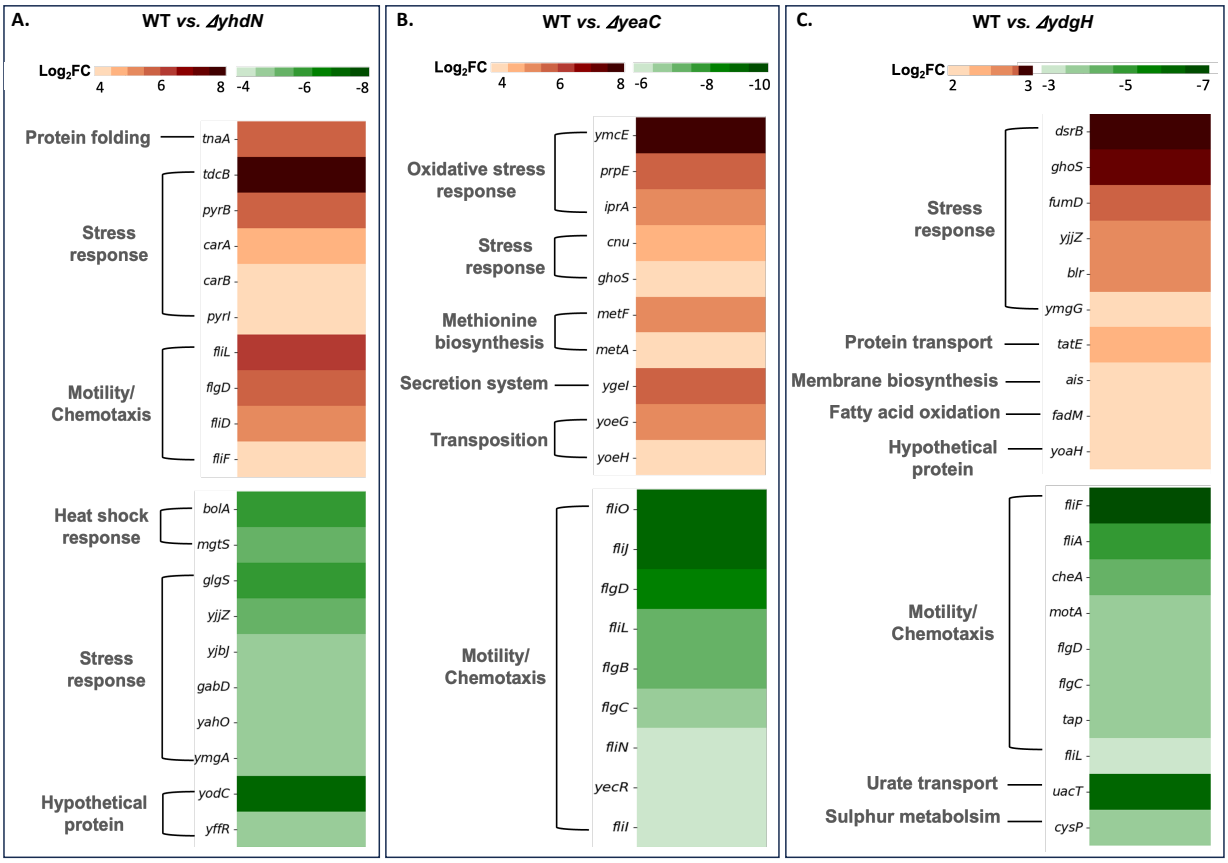

Figure 4. Comparative differential gene expression analysis in A. wild type (WT) *vs. ΔyhdN*, B. WT *vs. ΔyeaC* and C. WT *vs. ΔydgH* strains. Top ten positively and negatively expressed DEGs are shown. Each row represents a gene, and colour intensity represents the Log_2 Fold Change (Log2 FC), with red indicating upregulation in WT and green indicating upregulation in the mutant strains. Functional categories were based on information retrieved from Literature and EcoCyc.

Conclusion and Outlook

The functional characterization of hypothetical protein (HP)-encoding genes remains a critical challenge, since the rapid accumulation of sequencing data has long surpassed the rate of possible experimental characterization *in vivo* and *in vitro*. While there have been notable advancements in methodologies for protein function prediction in the recent past, several challenges persist, including the heavy reliance on pre-existing data inferred from model

516 organisms. Unfortunately, even in the best studied model organisms a significant amount of
517 protein encoding genes could so far not been annotated.
518
519 AI-driven approaches, such as machine learning (ML) algorithms, now offer powerful tools to
520 analyze vast omics datasets. In this study we employed a comprehensive approach,
521 integrating independent component analyses to decipher transcriptional regulatory networks,
522 deep learning for structural homolog prediction, and various other bioinformatic tools to
523 characterize HPs that have no functional information available in public databases. With this
524 methodology putative/probable functions for at least 64% of 95 hypothetical HPs encoding
525 genes from *E. coli* K-12 could be extrapolated, facilitating the subsequent functional validation
526 of these proteins through *in vitro* and *in vivo* experiments in the future. For the remaining 36%
527 HPs, however, more high-quality datasets including metabolomics and proteomics are
528 probably needed, as these genes are often seen to be expressed under very specific
529 environmental conditions from which only one dataset was available. Nevertheless, for most
530 proteins it is possible to derive at least some characteristics from their general sequence
531 properties, whether there is evidence of expression, their possible cellular location, details of
532 homologs, or whether they are predicted or demonstrated to be expressed as part of an
533 operon and/or regulon. Taking these information into account in databases will aid in the
534 improvement of using AI tools for annotation in the future.
535
536 In this study we furthermore provided an experimental feedback loop for three HP-encoding
537 genes to verify the *in silico* prediction. Gene *yhdN* ought to play a role in the cells' responding
538 to heat shock and nutrient limitation, which could be confirmed by comparing the growth
539 curves and transcriptional responses of wild type and *ΔyhdN* deletion mutant strains. For the
540 second candidate *yeaC, in silico* predictions suggested a role in aerobic respiration.
541 Experimental evidence supported this hypothesis by the upregulation of oxidative stress
542 response and methionine biosynthesis genes, hence it is likely involved in scavenging reactive
543 oxygen species. In contrast, the significant upregulation of "Motility"/Chemotaxis" genes in the

544 deletion mutant suggest that during the absence of *yeaC*, bacteria may enhance motility
545 pathways as an adaptive mechanism under oxidative stress. The third candidate *ydgH*, was
546 predicted *in silico* to play a role in oxidoreduction, which could also be confirmed by the *in vivo*
547 experiments showing its role in the protection against oxidative stress. Similar to *yeaC,* in the
548 mutant an upregulation of motility/chemotaxis genes indicate that in the absence of *ydgH*, the
549 cell may compensate for reduced oxidoreductive function. However, it is important to
550 acknowledge that our understanding still remains incomplete since the functional landscape
551 of proteins is vast and complex. Future studies and more omics datasets are needed to further
552 refine and expand upon our findings, exploring the broader implications of these proteins
553 under different environmental conditions.
554
555 In conclusion, this study represents a significant step forward in elucidating the functions of
556 previously uncharacterized HPs with no information in existing knowledge databases.
557 Leveraging AI-driven annotations and integrating them with experimental laboratory work will
558 link new functional roles of genes, discover previously unknown cellular and metabolic
559 processes and maybe even biotechnological potentials. In the future this approach might also
560 aid in the isolation of new and so far uncultured microbial species, i.e. microbial dark matter,
561 by harnessing meta-omics datasets and identifying genes critical for growth and adaptation,
562 offering clues to optimize culture conditions.
563
564
565
566 **Methods**
567 **Identification and enumeration of hypothetical proteins (HPs)**
568 For the comprehensive analysis of *Escherichia coli* K-12 (*E. coli*) substrains MG1655 and
569 BW25113, the complete genome sequences available in the NCBI RefSeq database under
570 the accession number GCF_000005845.2 and GCF_004355105.2 were used, respectively.
571 Ribosomal RNA (rRNA), transfer RNA (tRNA), non-coding RNA (ncRNA) were filtered out.

572 CDS based annotations were used to find hypothetical proteins (HPs). HPs were identified
573 based on keywords like “Putative”, “Putative uncharacterized”, “Uncharacterized protein” and
574 “DUF (domain of unknown function)-domain containing protein”, “UPF” (unknown protein
575 family) as well as proteins having a ‘Protein Y…’ pattern. Further information was extracted
576 from the extensively curated databases EcoCyc version 26.1 [39], RegulonDB version 11.2
577 [11], EggNOG v6.0 [12] and UniProt release 2023_04 for proteome UP000000625 [1].
578 In order for a HP to be classified as a protein with no characterization (target group of this
579 study), it had to fulfill all of the following criteria:

580 1. The **EcoCyc** protein summary showed the statement 'No information about this'.
581 Additionally, the protein had to be marked as ‘Uncharacterized’. Proteins which had
582 the statement but a ‘Partial’ characterization in EcoCyc were further investigated using
583 UniProt.
584 2. In **UniProt** the protein lacked any functional information in the 'Function' section and
585 was assigned an annotation score of '1', and a ‘protein existence’ score of ‘4’ signifying
586 that the protein, although predicted to be expressed, lacked information based on
587 experimental evidence or orthologs in closely related species. For the “Function”
588 section, a score of '1' is the lowest rating in a five-point-scoring system and for the
589 “protein existing” category a score of ‘4’ out of ‘5’, where ‘5’ indicates a higher level of
590 uncertainty regarding the protein's expression.
591 3. In the **RegulonDB** database it had the label “Weak” evidence for an annotation in the
592 evidence section and no additional information in the ‘Note’ subsection.
593 4. In the **EggNOG** database the protein was either classified under the cluster of
594 orthologous groups (COG) with a functional category 'S', where 'S' designates proteins
595 belonging to an unknown function category or it lacked an ortholog which was
596 displayed as ‘No orthologs found’.

597

598 95 of the 4403 *E. coli* K-12 protein encoding genes fulfilled these criteria. All scripts for the
599 filtering and enumeration of uncharacterized HPs can be found on Figshare

600 (*Notebooks>HP_curation*). In addition, the here identified HP-encoding genes were compared
601 with the ones identified by Ghatak et al. in 2019 [8] to check for their current status.
602
603 **Transcriptomic data curation and processing**
604 RNA-sequencing data from NCBI for analyzing the expression patterns of genes was collected
605 for *E. coli* K-12 substrains MG1655 and BW25113 using an adapted workflow for *Bacillus*
606 *subtilis* [32]. For substrain MG1655 1854 datasets and for substrain BW25113 662 datasets
607 were downloaded and processed. Raw FASTQ files were obtained using sratoolkit 3.0.1 [161],
608 and subsequent read trimming was performed using Trim Galore 0.6.5 [162] with the default
609 settings. Trimmed reads were then subjected to FastQC 0.11.9 [163]. Alignments to the
610 genomes were done using Bowtie 1.2.3 [164]. The read direction was determined using
611 RSeQC 3.0.1 [165] before generating read counts using featureCounts [166]. Finally, all
612 quality control metrics were compiled using MultiQC [167] and the expression compendium
613 was obtained as log-transformed Transcripts per Million (log-TPM) values. Quality metrics
614 were established to filter and ensure the selection of high-quality datasets with the following
615 modifications [168]: Briefly, the datasets were considered to be of high quality if they passed
616 the fastqc parameters 'per_base_sequence_quality', 'per_sequence_quality_scores',
617 'per_base_n_content', 'adapter_content' and had at least 500,000 reads mapped to coding
618 sequences from the reference genome. To preserve biological variability and prevent loss of
619 information, samples with no replicates were also retained in the dataset. Short non-coding
620 transcripts (<100 nucleotides) and extremely low-expression transcripts (Fragments Per
621 Kilobase per Million mapped reads < 10) were removed to reduce noise. 779 datasets for
622 substrain MG1655 and 135 datasets for substrain BW25113 were then used for further
623 analysis. All other information on the *E. coli* K-12 genes including their transcription units,
624 descriptions etc. were sourced from EcoCyc by utilizing the SmartTables feature [39].
625 Annotations for clusters of orthologous groups (COG) were obtained from EggNOG v6.0 [12]
626 including Gene Ontology [169]. The transcriptional regulatory network (TRN) comprising
627 information on genes and their governing regulators (i.e. transcription factors controlling the

628 expression of genes) were sourced from RegulonDB version 12.0 [11] and EcoCyc [39] as
629 described by Sastry et al. [32] In order to mitigate any batch effects which might be caused
630 due to the usage of diverse datasets, a reference condition (wild type *E. coli* K-12 substrain
631 MG1655 in M9 minimal medium facilitated with glucose and essential micronutrients under
632 non-stressful conditions) was used [30]. This was done by subtracting the mean expression
633 of two replicates of the chosen reference condition from the entire gene expression dataset
634 and calculating the log2-fold-change i.e. relative changes in expression. This normalization
635 method allowed for the comparison of gene expression differences relative to a common
636 baseline as previously demonstrated in Sastry et al. [30]. The normalized data was then used
637 as input for machine learning (*Data processing>Nextflow*).
638
639 **Independent Component Analysis of Transcriptomic Data**
640 Independent Component Analysis (ICA) developed by McCon et al. -named OptICA- was
641 applied to prevent both over-decomposition and under-decomposition of transcriptomic
642 datasets [27]. The application of ICA to the normalized *E. coli* K-12 substrain MG1655 RNAseq
643 data resulted in two matrices: the first matrix, denoted as the M matrix, encompassing the
644 robust independent components named iModulons, while the second matrix, termed the A
645 matrix, comprised the corresponding activities of iModulons over different growth conditions.
646 Additionally, a PyModulon package was used in conjunction with Jupyter notebooks to
647 characterize the iModulons [32]. The scripts containing the specific utilization of resources and
648 curation of iModulons can be found on Figshare (*OptICA* and *iModulon curation*). The
649 information from substrain MG1655 was then used to infer the iModulons and their member
650 genes for substrain BW25113, since only for the latter strain single-gene deletion mutants
651 were available for *in vitro* experimentation. The HP-encoding genes, the regulators governing
652 them, and their derived functions can be found in **Table 1.**
653
654 Possible functions for the 95 HP-encoding genes were further identified through regulators
655 governing their gene expression, as provided by RegulonDB and EcoCyc and/or by Gene

656 Ontology (GO) terms derived from co-regulating genes using the PANTHER (Protein ANalysis
657 THrough Evolutionary Relationships) tool [33]. Here, member genes of an iModulon (including
658 the gene of interest, i.e. the HP-encoding gene) were used as input to obtain GO terms to see
659 if any were overrepresented. Statistically significant GO categories with the default false
660 Discovery Rate (FDR)-adjusted p-value (<0.05) were manually identified for each HP
661 (*Supplementary Table 1*). These gene-associated functional categories can be found in **Table**
662 **1** and **Figure 2**.
663
664 **Metadata extraction**
665 Metadata conditions for all datasets were retrieved either manually from the sequence read
666 archive (SRA), *via* a semi-automated approach [167] or by utilizing data from the Gene
667 Expression Omnibus Database using the GEOparse tool [170] to obtain experimental
668 information not available *via* the NCBI's Entrez Programming Utilities (E-utilities) [42]. As a
669 result, from 779 quality checked datasets for the substrain MG1655, metadata for 602 datasets
670 could be retrieved with confidence and termed as 'Explicit metadata'. 113 datasets were
671 termed as 'poor metadata', meaning that information on one or more experimental conditions
672 (such as media composition, temperature, pH, etc.) was missing or incomplete. Lastly,
673 datasets with 'unclear metadata' lacked all information. For the substrain BW25113, 128
674 datasets were 'Explicit' while seven were 'unclear' (*Notebooks>metadata_curation*).
675 Additionally, metadata condition for the highest expression of the HP- encoding genes against
676 the reference gene *frr* were extracted from the Tjaden dataset [44] in order to account for the
677 loss of datasets after quality filtering (also see below). The *frr* gene expression is typically
678 consistent across different conditions which was also observed when tested as reference
679 along with other genes like *rpoC*, *rpoD* for the uncharacterized HPs [this study, 171]. Hence,
680 gene *frr* was chosen as the reference gene serving as a control to validate the relative
681 expression levels of other genes. The extensive nature of this dataset ensured a broad
682 representation of gene expression profiles, in addition to the datasets procured for OptICA
683 analysis (*Notebooks> metadata_curation*).

684

685 **Co-expression analysis based on public RNA-Seq data**

686 To identify genes with expression patterns similar to those encoding HPs, a Spearman
687 correlation analysis on the Tjaden dataset was performed [172]. This dataset comprises a
688 comprehensive collection of 3.376 *E. coli* strain K-12 RNA-seq datasets, with expression
689 levels quantified in transcripts per million (TPM) [44]. For inferring gene-gene correlations
690 across the transcriptomic datasets for strain *E. coli* K-12, we identified the top ten co-
691 expressed genes to the respective 95 HP-encoding gene and used this information to get an
692 inference on their functions [10] **(Table 1)** (*Notebooks>gene_co-expression*).

693

694 **Sub-Cellular Localization**

695 For the purpose of determining the subcellular localizations of the 95 HP-encoding genes,
696 BUSCA (Bologna Unified Subcellular Component Annotator) was employed [173]. This tool
697 integrates various machine learning and bioinformatics tools [174–177] to analyze and
698 recognize patterns in protein sequences that are indicative of specific subcellular localizations.
699 The integrative webserver was used to obtain labels such as 'Nucleus', 'Periplasm/cytoplasm',
700 'Inner/outer membrane' or 'extracellular space'. All 95 HP-encoding genes with their predicted
701 sub-cellular localizations can be found in **Table1**.

702

703 **Protein-Protein Interactions (PPIs) Analysis**

704 The STRING database (version 12.0) (https://string-db.org) was employed for the
705 identification of PPIs of HP-encoding genes against the proteomic landscape of *E. coli*. The
706 tool incorporates data from diverse origins such as available publications, empirical evidence,
707 predictions derived from co-expression patterns, genomic context analysis, and curated
708 pathway databases. A 'confidence score' for each inferred association was derived,
709 quantitatively expressing the robustness of the predicted interaction [178]. In order to keep
710 only the high-scoring associations, a cut-off of 0.7 was utilized [179]. All 95 HP-encoding
711 genes and their interacting partner proteins are listed in **Table 1**.

712

713 **Analysis of Gene Context**

714 Shared functional relationships were analyzed using the genomic context of
715 *E. coli* strain K-12 (*Supplementary Figure 1*), particularly the genes located upstream and
716 downstream of the 95 genes of interest. A gene list comprising of gene names was used to
717 create a SmartTable in the EcoCyc database to examine the local genomic neighbourhood
718 and visualize the genes upstream and downstream, including their orientations [36]. (**Table**
719 **1)**.

720

721 **Detection of Remote Protein Homology**

722 In order to identify distantly homologous sequences, HP sequences were used as input for
723 the HHblits tool (version 3.3.0) available in the MPI Bioinformatics Toolkit using a Hidden
724 Markov Model (HMM) iterative sequence search [180]. The HHblits server
725 (https://toolkit.tuebingen.mpg.de/tools/hhblits) takes a single sequence or a multiple sequence
726 alignment as input and iteratively searches through the selected HMM databases [181,182].
727 HHblits performs sequence search and remote homology detection with higher sensitivity as
728 compared to gold-standard databases like InterPro [180]. Homologous sequences were then
729 searched against the default UniRef30 database [37]. Sequence based remote homologies
730 identified through the HHblits tool are catalogued in **Table 1**.

731

732 **Structure-Based Homology**

733 For identifying structural homologs, we used the AlphaFold Protein Structure Database
734 (AFDB) (https://cluster.foldseek.com/), a specialized computational database that includes
735 structural models for approximately 215 million protein sequences. This platform employs
736 deep learning algorithms to scan and match protein structures, enabling the discovery of
737 structural similarities, even among proteins with low sequence identity [183]. We analyzed
738 clusters to perform comparisons of HPs with all protein structures in the AFDB. UniProt

739 accession IDs were used as inputs to identify the cluster to which the HP belongs. The
740 homology-based function information for each of the 95 HP is listed in **Table 1**. A script to
741 extract the information can be found on Figshare (*Notebooks> HP_info_curation*).
742
743 **Bacterial strains and growth conditions**
744 *E. coli* K-12 substrain BW25113 was sourced from Horizon Discovery Ltd., United States.
745 Three single-gene knockout mutants from *E. coli* strain K-12 substrain BW25113 *ΔyhdN,*
746 *ΔyeaC*, and *ΔydgH* were obtained from the KEIO collection (NBRP, Japan). Glycerol stocks
747 were stored in an ultra-low temperature freezer (Thermo Fisher, United States) at −80°C until
748 further processing. Cells were cultured overnight on agar plates from glycerol stocks and
749 single colonies were picked from the agar plate and then used to Luria Bertani (LB) liquid
750 medium at 37°C [184].
751
752
753
754 **Media and reagents**
755 *E. coli* strains were cultured in LB broth (10 g/L tryptone, 5 g/L yeast extract, and 10 g/L NaCl;
756 pH 7.0) at 37°C while shaking at 200 rpm [184]. M9 liquid medium for the pre-culture was
757 prepared using 42 mM Na_2HPO_4, 22 mM KH_2PO_4, 8.5 mM NaCl, 18.7 mM NH_4Cl, 2 mM
758 $MgSO_4$, 0.1 mM $CaCl_2$ and 11 mM glucose, supplemented with 0.05% casamino acids to
759 ensure non-limiting conditions. For nitrogen limited M9 medium, a NH_4Cl concentration of 0.16
760 mM was used without the addition of casamino acids. For solid medium, 1.5% agar was
761 added. 30% H_2O_2 was sterile filtered through a 0.22 μm pore size filter to ensure sterility prior
762 to be used in the oxidative stress experiments. For all experiments with H_2O_2 the LB was
763 freshly prepared and kept in the dark until use. All chemicals were sourced from Sigma
764 Chemical Co. (St. Louis, MO, USA).
765
766 **Measurement of Bacterial Growth Curves**

767 Bacterial cultures were inoculated at a 1:100 dilution unless stated otherwise. Each
768 experiment included triplicates. All optical density values (OD_{600}) were measured *via* a cell
769 density meter (Ultrospec 10, biochrom). OD_{600} was measured every 2h for heat shock in LB
770 and M9 or M9 modified medium and every 1h for oxidative stress experiments. Growth curves
771 were generated for each set of experiments including the wild type and mutant strain in
772 stressed and non-stressed conditions (controls).
773
774 Heat stress
775 A single colony (wild type and Δ*yhdN*) was picked from either LB or M9 agar plates and
776 inoculated into 5 mL LB broth for overnight cultivation at 37°C and shaken with 200 rpm. The
777 overnight culture was then used to inoculate fresh LB medium at a 1:100 dilution, which was
778 then cultured for ~2-3h at 37°C and 200 rpm until an OD_{600} of 0.4 was reached. This was
779 repeated with the M9 liquid medium (preculture), at 37°C to ensure non limiting conditions.
780 For the nitrogen limitation assay, medium was prepared using 0.16mM NH_4Cl. To study the
781 effects of heat shock on bacterial growth, the culture was grown to mid-log phase (OD_{600} 0.4),
782 diluted to OD_{600} 0.04 and then heat shocked for 7 minutes in a shaker-incubator at 50°C. After
783 treatment, the bacterial suspension was incubated for 12 h at 37°C. Samples were measured
784 every 2h for 12h.
785
786 Oxidative stress
787 For studying the effects of oxidative stress, a single colony (wild type, *ΔyeaC* and *ΔydgH*) was
788 picked from the LB agar plate and inoculated into 5 mL LB for overnight cultivation at 37°C
789 and shaken with 200 rpm. The overnight culture was then used to inoculate fresh LB (dilution
790 of 1:100) and cultured at 37°C and 200 rpm until an OD_{600} of 0.2 was reached. An OD of 0.2
791 was used since at this stage the cells were actively dividing, making them susceptible to the
792 effects of oxidative stress, allowing for better characterization and analysis of the stress
793 response[137]. H_2O_2 was added at a final concentration of 2.5 mM. After treatment, the
794 bacterial suspension was incubated for 5h at 37°C and the OD_{600} was measured hourly.

795

796 **RNA Sequencing and data processing**

797 2 ml of cell suspension from the heat shock samples was collected after 2h and 6h of growth.
798 For the oxidative stress experiments, samples were collected after 1h and 5h of growth. The
799 medium was discarded, cell pellets were washed with Phosphate Buffer Saline and mixed with
800 DNA/RNA shield™ (Zymo Research Corp., Freiburg, Germany). All samples were processed
801 according to the manufacturer's instructions. Samples were preserved at -20°C until RNA
802 extraction. RNA was extracted using the Direct-zol RNA Miniprep Plus Kit (Zymo Research
803 Corp., Freiburg, Germany) according to the manufacturer's instructions. Total RNA was eluted
804 from columns with 100 µL nuclease-free water and quantified using the Qubit RNA Broad
805 Range Assay Kit (Thermo Fisher Scientific Inc., Waltham, MA, USA). The quality was
806 assessed by running an RNA-nano chip on an Agilent bioanalyzer (Agilent Technologies,
807 Waldbronn, Germany). Samples with an RNA integrity score ≥8 were used for further
808 processing [185]. The rRNA was removed from total RNA preparations using the NEBNext
809 rRNA Depletion (Bacteria) kit (New England Biolabs, Frankfurt, Germany). Paired-end library
810 preparation was done using the NEBNext Ultra II Directional RNA Library Prep Kit for Illumina
811 (New England Biolabs, Frankfurt, Germany) following the manufacturer's instructions with an
812 average insert size of 200 bp. Libraries were run on a NextSeq 550™ (Illumina, San Diego,
813 CA, United States).

814

815 The RNAflow pipeline [186] was implemented using a conda environment. Sequence reads
816 were checked for quality using FastQC v0.11.9 [187]. Raw reads were processed using fastp
817 v0.20.0 [188], which employs a sliding window approach for quality trimming and adapter
818 clipping, with the settings: a -5 to -3 cut for front and tail, a default window of 4 and mean
819 quality threshold of 20. Trimmed reads shorter than 15 bps were discarded. The remaining
820 reads were mapped onto the *E. coli* K-12 reference genome (NZ_CP009273.1) using HISAT
821 v2.1.0 [189]. The generated output was converted into a BAM format using samtools-1.20
822 [190], followed by the processes of sorting and indexing. A gene transfer format (GTF)

823 annotation file for *E. coli* substrain BW25113 was used to filter for gene and pseudogene
824 features. FeatureCounts v2.0.1 [191] was used to quantify the mapped reads based on the
825 gene annotations. Processed datasets were summarized in a MultiQC v1.9 [167] generated
826 file. were normalized by the DESeq2 module (v1.28.0) in R (version 4.3.2) using a
827 variance stabilizing transformation [192].
828
829 **Comparative gene expression analysis of wild type and isogenic mutant strains**
830 Sequencing reads were obtained from the transcriptomic datasets of wild-type (WT), *ΔyhdN*,
831 *ΔyeaC,* and *ΔydgH* mutants, respectively. Non-stressed control and heat shocked samples
832 from WT and *ΔyhdN* at the 6h timepoint and non-stressed control and oxidative stress samples
833 from WT, *ΔyeaC,* and *ΔydgH* at the 5h timepoint were used to identify up- or downregulated
834 genes. DESeq2 [192] was utilized to examine expression differences of genes in the WT and
835 mutant strains under both control and stress conditions. To focus on the specific effect of
836 stress on gene expression rather than the difference of WT *vs.* deletion mutants, read counts
837 under control conditions were subtracted from the read counts under stress condition [193].
838 Genes with an adjusted P-value (Padj) of 0.1 or less were classified as differentially expressed
839 to avoid false positives. A cut-off $\log_2$ fold change ($\log_2$FC) of 1.5 was chosen for further
840 analysis [194]. A $\log_2$FC of 1.5 means that a gene was 2.83 times more expressed in one
841 strain *vs.* the other, a $\log_2$FC of 2 means that a gene was 4 times more expressed and so on.
842 Significant positive $\log_2$FC indicated genes that were upregulated in WT relative to the mutant,
843 while negative values showed an upregulation in the mutant *vs*. WT. To determine the
844 functional categories of these genes, the EcoCyc database was used [36]. Information of the
845 differentially expressed genes can be found on Figshare (*DEGs>Table1*).
846
847 **Data availability**
848 All code and scripts used in this study are available on Figshare. These resources can be
849 accessed at https://figshare.com/s/0ede175c510cf201e7c2.

Raw sequencing data that supports the findings of this study have been deposited in the Sequence Read Archive with the BioProject ID: PRJNA1209969.

Competing interests

The authors declare that they have no conflict of interest.

Funding

This work was supported by the Karlsruhe Institute of Technology and the Helmholtz Society [POF4; 5207.0004.0012].

Authors' contributions

S.C, H.A. and Z.A did the data analyses, S.C. did the *in vitro* experiments, S.C and A.K.K. wrote the manuscript, A.K.K. provided the funding.

Acknowledgements

The authors acknowledge the support by the state of Baden-Württemberg through bwHPC. We thank Dr. Gunnar Sturm for technical support and insightful discussions and David Thiele for library preparation assistance.

References

1. Consortium TU. UniProt: the Universal Protein Knowledgebase in 2023. Nucleic Acids Res. 2023;51:D523–31; doi:10.1093/nar/gkac1052

2. Paysan-Lafosse T, Blum M, Chuguransky S, Grego T, Pinto BL, Salazar GA, et al. InterPro in 2022. Nucleic Acids Res. 2023;51:D418–27; doi:10.1093/nar/gkac993

3. Mistry J, Chuguransky S, Williams L, Qureshi M, Salazar GA, Sonnhammer ELL, et al. Pfam: The protein families database in 2021. Nucleic Acids Res. 2021;49:D412–9; doi:10.1093/nar/gkaa913

4. Sigrist CJA, de Castro E, Cerutti L, Cuche BA, Hulo N, Bridge A, et al. New and continuing developments at PROSITE. Nucleic Acids Res. 2013;41:D344–7; doi:10.1093/nar/gks1067

5. Letunic I, Khedkar S, Bork P. SMART: recent updates, new developments and status in 2020. Nucleic Acids Res. 2021;49:D458–60; doi:10.1093/nar/gkaa937

6. Lu S, Wang J, Chitsaz F, Derbyshire MK, Geer RC, Gonzales NR, et al. CDD/SPARCLE: the conserved domain database in 2020. Nucleic Acids Res. 2020;48:D265–8; doi:10.1093/nar/gkz991

7. Durairaj J, Waterhouse AM, Mets T, Brodiazhenko T, Abdullah M, Studer G, et al. Uncovering new families and folds in the natural protein universe. Nature. 2023;622:646–53; doi:10.1038/s41586-023-06622-3

8. Ghatak S, King ZA, Sastry A, Palsson BO. The y-ome defines the 35% of *Escherichia coli* genes that lack experimental evidence of function. Nucleic Acids Res. 2019;47:2446–54; doi:10.1093/nar/gkz030

9. Ardern Z, Chakraborty S, Lenk F, Kaster A-K. Elucidating the functional roles of prokaryotic proteins using big data and artificial intelligence. FEMS Microbiol Rev. 2023;47; doi:10.1093/femsre/fuad003

10. Keseler IM, Gama-Castro S, Mackie A, Billington R, Bonavides-Martínez C, Caspi R, et al. The EcoCyc Database in 2021. Front Microbiol. 2021;12; doi:10.3389/fmicb.2021.711077

11. Salgado H, Gama-Castro S, Lara P, Mejia-Almonte C, Alarcón-Carranza G, López-Almazo AG, et al. RegulonDB v12.0: a comprehensive resource of transcriptional regulation in *E. coli* K-12. Nucleic Acids Res. 2024;52:D255–64; doi:10.1093/nar/gkad1072

12. Hernández-Plaza A, Szklarczyk D, Botas J, Cantalapiedra CP, Giner-Lamia J, Mende DR, et al. eggNOG 6.0: enabling comparative genomics across 12 535 organisms. Nucleic Acids Res. 2023;51:D389–94; doi:10.1093/nar/gkac1022

13. Mills CL, Beuning PJ, Ondrechen MJ. Biochemical functional predictions for protein structures of unknown or uncertain function. Comput Struct Biotechnol J. 2015;13:182–91; doi:10.1016/j.csbj.2015.02.003

14. Zhang C, Freddolino PL, Zhang Y. COFACTOR: improved protein function prediction by combining structure, sequence and protein–protein interaction information. Nucleic Acids Res. 2017;45:W291–9; doi:10.1093/nar/gkx366

15. Makrodimitris S, van Ham RCHJ, Reinders MJT. Improving protein function prediction using protein sequence and GO-term similarities. Bioinformatics. 2019;35:1116–24. Available from: doi:10.1093/bioinformatics/bty751

16. Saha S, Chatterjee P, Basu S, Nasipuri M, Plewczynski D. FunPred 3.0: improved protein function prediction using protein interaction network. PeerJ. 2019;7. doi: 10.7717/peerj.6830

17. Varadi M, Tsenkov M, Velankar S. Challenges in bridging the gap between protein structure prediction and functional interpretation. Proteins: Structure, Function, and Bioinformatics. 2023; doi:10.1002/prot.26614

18. Vincent AT. Bacterial hypothetical proteins may be of functional interest. Frontiers in Bacteriology. 2024;3; doi:10.3389/fbrio.2024.1334712

19. Jeffery CJ. Current successes and remaining challenges in protein function prediction. Frontiers in Bioinformatics. 2023;3; doi:10.3389/fbinf.2023.1222182

20. Pavlopoulos GA, Baltoumas FA, Liu S, Selvitopi O, Camargo AP, Nayfach S, et al. Unraveling the functional dark matter through global metagenomics. Nature. 2023;622:594–602; doi:10.1038/s41586-023-06583-7

21. Escudeiro P, Henry CS, Dias RPM. Functional characterization of prokaryotic dark matter: the road so far and what lies ahead. Curr Res Microb Sci. 2022;3:100159; doi: 10.1016/j.crmicr.2022.100159

22. da Costa WLO, Araújo CL de A, Dias LM, Pereira LC de S, Alves JTC, Araújo FA, et al. Functional annotation of hypothetical proteins from the *Exiguobacterium antarcticum* strain B7 reveals proteins involved in adaptation to extreme environments, including high arsenic resistance. PLoS One. 2018;13:e0198965; doi:10.1371/journal.pone.0198965

23. Grünberger F, Knüppel R, Jüttner M, Fenk M, Borst A, Reichelt R, et al. Exploring prokaryotic transcription, operon structures, rRNA maturation and modifications using Nanopore-based native RNA sequencing. bioRxiv. 2020;2019.12.18.880849; doi: 10.1101/2019.12.18.880849

24. Dall'Alba G, Casa PL, Abreu FP de, Notari DL, de Avila e Silva S. A Survey of Biological Data in a Big Data Perspective. Big Data. 2022;10:279–97; doi:10.1089/big.2020.0383

25. Chen J, Gu Z, Lai L, Pei J. In silico protein function prediction: the rise of machine learning-based approaches. 2023;3:487–510; doi:10.1515/mr-2023-0038

26. Alteri CJ, Lindner JR, Reiss DJ, Smith SN, Mobley HLT. The broadly conserved regulator PhoP links pathogen virulence and membrane potential in *Escherichia coli*. Mol Microbiol. 2011;82:145–63; doi:10.1111/j.1365-2958.2011.07804.x

27. Mcconn JL, Lamoureux CR, Poudel S, Palsson BO, Sastry A V. Optimal dimensionality selection for independent component analysis of transcriptomic data; doi:10.1186/s12859-021-04497-7

28. Yu J, Li M, Wang J, Hamushan M, Jiang F, Wang B, et al. Identification of *Staphylococcus aureus* virulence-modulating RNA from transcriptomics data with machine learning. Virulence. 2023;14:2228657; doi:10.1080/21505594.2023.2228657

29. Comon P. Independent component analysis, A new concept? Signal Processing. 1994;36:287–314; doi:10.1016/0165-1684(94)90029-9

30. Sastry A V, Gao Y, Szubin R, Hefner Y, Xu S, Kim D, et al. The *Escherichia coli* transcriptome mostly consists of independently regulated modules. Nat Commun. 2019;10:5536; doi:10.1038/s41467-019-13483-w

31. Sastry A V, Poudel S, Rychel K, Yoo R, Lamoureux CR, Chauhan S, et al. Title Mining all publicly available expression data to compute dynamic microbial transcriptional regulatory networks Authors; doi:10.1101/2021.07.01.450581

32. Rychel K, Sastry A V., Palsson BO. Machine learning uncovers independently regulated modules in the *Bacillus subtilis* transcriptome. Nat Commun. 2020;11. doi: 10.1038/s41467-020-20153-9

33. Thomas PD, Ebert D, Muruganujan A, Mushayahama T, Albou L-P, Mi H. PANTHER: Making genome-scale phylogenetics accessible to all. Protein Science. 2022;31:8–22; doi:10.1002/pro.4218

34. Savojardo C, Martelli PL, Fariselli P, Profiti G, Casadio R. BUSCA: an integrative web server to predict subcellular localization of proteins. Nucleic Acids Res. 2018;46:W459–66; doi:10.1093/nar/gky320

35. Szklarczyk D, Kirsch R, Koutrouli M, Nastou K, Mehryary F, Hachilif R, et al. The STRING database in 2023: protein–protein association networks and functional enrichment analyses for any sequenced genome of interest. Nucleic Acids Res. 2023;51:D638–46; doi: 10.1093/nar/gkac1000

36. D KP, Suzanne P, Ron C, Anamika K, Markus K, E MP, et al. The EcoCyc Database (2023). EcoSal Plus. 2023;11:eesp-0002-2023; doi:10.1128/ecosalplus.esp-0002-2023

37. Gabler F, Nam S-Z, Till S, Mirdita M, Steinegger M, Söding J, et al. Protein Sequence Analysis Using the MPI Bioinformatics Toolkit. Curr Protoc Bioinformatics. 2020;72:e108; doi:10.1002/cpbi.108

38. Barrio-Hernandez I, Yeo J, Jänes J, Mirdita M, Gilchrist CLM, Wein T, et al. Clustering predicted structures at the scale of the known protein universe. Nature. 2023;622:637–45; doi:10.1038/s41586-023-06510-w

39. Karp PD, Billington R, Caspi R, Fulcher CA, Latendresse M, Kothari A, et al. The BioCyc collection of microbial genomes and metabolic pathways. Brief Bioinform. 2019;20:1085–93; doi:10.1093/bib/bbx085

40. Choudhary S. pysradb: A Python package to query next-generation sequencing metadata and data from NCBI Sequence Read Archive. F1000Res. 2019;8:532; doi: 10.12688/f1000research.18676.1

41. Gumienny R. GEOparse. Rev.0a257463. 2015. Available from: https://geoparse.readthedocs.io/en/latest/

42. Liu M, Durfee T, Cabrera JE, Zhao K, Jin DJ, Blattner FR. Global transcriptional programs reveal a carbon source foraging strategy by *Escherichia coli*. J Biol Chem. 2005;280:15921–7; doi: 10.1074/jbc.m414050200

43. Tjaden B. *Escherichia coli* transcriptome assembly from a compendium of RNA-seq data sets. RNA Biol. 2023;20:77–84; doi:10.1080/15476286.2023.2189331

44. Rawangkan A, Yosboonruang A, Kiddee A, Siriphap A, Pook-In G, Praphasawat R, et al. Restoring Ampicillin Sensitivity in Multidrug-Resistant *Escherichia coli* Following Treatment in Combination with Coffee Pulp Extracts. J Microbiol Biotechnol. 2023;33:1–10; doi:10.4014/jmb.2304.04051

45. Manat G, El Ghachi M, Auger R, Baouche K, Olatunji S, Kerff F, et al. Membrane Topology and Biochemical Characterization of the *Escherichia coli* BacA Undecaprenyl-Pyrophosphate Phosphatase. PLoS One. 2015;10:e0142870; doi:10.1371/journal.pone.0142870

46. Hajra D, Nair AV, Chakravortty D. An elegant nano-injection machinery for sabotaging the host: Role of Type III secretion system in virulence of different human and animal pathogenic bacteria. Phys Life Rev. 2021;38:25–54; doi:10.1016/j.plrev.2021.05.007

47. Prakash A, Dutta D. Bicyclomycin generates ROS and blocks cell division in *Escherichia coli*. PLoS One. 2024;19:e0293858; doi:10.1371/journal.pone.0293858

48. Ogawa A, Kojima F, Miyake Y, Yoshimura M, Ishijima N, Iyoda S, et al. Regulation of constant cell elongation and Sfm pili synthesis in *Escherichia coli* via two active forms of FimZ orphan response regulator. Genes to Cells. 2022;27:657–74; doi:10.1111/gtc.12982

49. Lamark T, Røkenes TP, McDougall J, Strøm AR. The complex bet promoters of *Escherichia coli*: regulation by oxygen (ArcA), choline (BetI), and osmotic stress. J Bacteriol. 1996;178(6):1655–62; doi:10.1128/jb.178.6.1655-1662.1996.

50. Kambampati R, Lauhon CT. Evidence for the Transfer of Sulfane Sulfur from IscS to ThiI during the in Vitro Biosynthesis of 4-Thiouridine in *Escherichia coli* tRNA*. Journal of Biological Chemistry. 2000;275:10727–30; doi:10.1074/jbc.275.15.10727

51. Laura F-G, Xinyu G, Joy K, Sooyeon S, E BM, Rodolfo G-C, et al. Single-cell analysis reveals that cryptic prophage protease LfgB protects *Escherichia coli* during oxidative stress by cleaving antitoxin MqsA. Microbiol Spectr. 2024;12:e03471-23; doi:10.1128/spectrum.03471-23

52. Zorraquino-Salvo V, Quinones-Soto S, Kim M, Rai N, Tagkopoulos I. Deciphering the genetic and transcriptional basis of cross-stress responses in *Escherichia coli* under complex evolutionary scenarios. bioRxiv. 2014;010595; doi:

53. May T, Okabe S. Enterobactin is required for biofilm development in reduced-genome *Escherichia coli*. Environ Microbiol. 2011;13:3149–62; doi:10.1111/j.1462-2920.2011.02607.x

54. Saier Jr MH, Reddy VS, Tamang DG, Västermark Å. The Transporter Classification Database. Nucleic Acids Res. 2014;42:D251–8; doi:10.1093/nar/gkt1097

55. Muto A, Goto S, Kurita D, Ushida C, Soma A, Himeno H. A leaderless mRNA including tRNA-like sequence encodes a small peptide that regulates the expression of GcvB small RNA in *Escherichia coli*. The Journal of Biochemistry. 2022;171:459–65; doi:10.1093/jb/mvac007

56. Njenga R, Boele J, Öztürk Y, Koch H-G. Coping with stress: How bacteria fine-tune protein synthesis and protein transport. Journal of Biological Chemistry. 2023;299:105163; doi: 10.1016/j.jbc.2023.105163

57. Rodríguez-Ochoa JI, Fragoso-Jiménez JC, Flores N, et al. Global transcriptomic response of *Escherichia coli* to p-coumaric acid. Microb Cell Fact. 2022;21:148; doi:10.1186/s12934-022-01874-6.

58. Bak G, Lee J, Suk S, Kim D, Lee J, Kim K, et al. Identification of novel sRNAs involved in biofilm formation, motility, and fimbriae formation in *Escherichia coli*. Sci Rep. 2015;5:15287; doi:10.1038/srep15287

59. Duarte-Velázquez I, Mora J, Ramírez-Prado J, Aguillón-Bárcenas A, Tornero-Gutiérrez F, Cordero-Loreto E, et al. *Escherichia coli* transcription factors of unknown function: sequence features and possible evolutionary relationships. PeerJ. 2022;10:e13772; doi:10.7717/peerj.13772

60. Saier Jr MH, Reddy VS, Tsu B V, Ahmed MS, Li C, Moreno-Hagelsieb G. The Transporter Classification Database (TCDB): recent advances. Nucleic Acids Res. 2016;44:D372–9; doi:10.1093/nar/gkv1103

61. Su C-C, Rutherford DJ, Yu EW. Characterization of the multidrug efflux regulator AcrR from *Escherichia coli*. Biochem Biophys Res Commun. 2007;361:85–90; doi:10.1016/j.bbrc.2007.06.175

62. Börner J, Friedrich T, Bartkuhn M, Klug G. Ribonuclease E strongly impacts bacterial adaptation to different growth conditions. RNA Biol. 2023;20:120–35; doi:10.1080/15476286.2023.2195733

63. A JN, Melissa F, E FS. Disruption of trehalose periplasmic recycling dysregulates cAMP-CRP signaling in *Escherichia coli* during stationary phase. J Bacteriol. 2023;205:e00292-23; doi:10.1128/jb.00292-23

64. Wang M, Fang K, Hong SMC, Kim I, Jang I-S, Hong SH. Medium chain unsaturated fatty acid ethyl esters inhibit persister formation of *Escherichia coli* via antitoxin HipB. Appl Microbiol Biotechnol. 2018;102:8511–24; doi:10.1007/s00253-018-9271-3

65. Muenter MM, Aiken A, Akanji JO, Baig S, Bellou S, Carlson A, et al. The response of *Escherichia coli* to the alkylating agents chloroacetaldehyde and styrene oxide. Mutation Research/Genetic Toxicology and Environmental Mutagenesis. 2019;840:1–10; doi:10.1016/j.mrgentox.2019.02.001

66. Hideji Y, Yasushi M, Shou F, Akiko S, Masami U, Akira W. YqjD Is an Inner Membrane Protein Associated with Stationary-Phase Ribosomes in *Escherichia coli*. J Bacteriol . 2012;194:4178–83; doi:10.1128/jb.00396-12

67. Hemm MR, Paul BJ, Schneider TD, Storz G, Rudd KE. Small membrane proteins found by comparative genomics and ribosome binding site models. Mol Microbiol. 2008;70:1487–501; doi:10.1111/j.1365-2958.2008.06495.x

68. Skjold AC, Ezekiel DH. Analysis of lambda insertions in the fucose utilization region of *Escherichia coli* K-12: use of lambda *fuc* and lambda *argA* transducing bacteriophages to partially order the fucose utilization genes. J Bacteriol. 1982;152:120–5; doi:10.1016/j.mrgentox.2019.02.001

69. Manuel C, Teresa ZM, Blas B, Gonzalo D-R, F JJ, Andrés VJ, et al. Anaerobic Catabolism of Aromatic Compounds: a Genetic and Genomic View. Microbiology and Molecular Biology Reviews. 2009;73:71–133; 10.1128/mmbr.00021-08

70. Arnim W, A KS, Kirsten J. Time-Dependent Proteome Alterations under Osmotic Stress during Aerobic and Anaerobic Growth in *Escherichia coli*. J Bacteriol. 2006;188:7165–75; doi:10.1128/jb.00508-06

71. Teufel R, Mascaraque V, Ismail W, Voss M, Perera J, Eisenreich W, et al. Bacterial phenylalanine and phenylacetate catabolic pathway revealed. Proc Natl Acad Sci U S A. 2010;107(32):14390–5; doi: 10.1073/pnas.1005399107.

72. Tenorio E, Saeki T, Fujita K, Kitakawa M, Baba T, Mori H, et al. Systematic characterization of *Escherichia coli* genes/ORFs affecting biofilm formation. FEMS Microbiol Lett. 2003;225(1):107–14; doi:10.1016/S0378-1097(03)00507-X.

73. Rodríguez-Montelongo L, Volentini SI, Farías RN, Massa EM, Rapisarda VA. The Cu(II)-reductase NADH dehydrogenase-2 of *Escherichia coli* improves the bacterial growth in extreme copper concentrations and increases the resistance to the damage caused by copper and hydroperoxide. Arch Biochem Biophys. 2006;451:1–7; doi:10.1016/j.abb.2006.04.019

74. Harwani D. Regulation of Gene Expression: Cryptic β-glucoside (bgl) Operon of *Escherichia coli* as a Paradigm. Brazilian Journal of Microbiology. 2014; doi:10.1590/S1517-83822014000400003

75. Anne P, K BI, Aurora L-N, F GJ, Valérie de C-L, D HA. FolX and FolM Are Essential for Tetrahydromonapterin Synthesis in *Escherichia coli* and Pseudomonas aeruginosa. J Bacteriol. 2010;192:475–82; doi:10.1128/jb.01198-09

76. Kotaka Y, Hashimoto M, Lee K, Kato J. Mutations identified in engineered *Escherichia coli* with a reduced genome. Front Microbiol. 2023;14; doi:10.3389/fmicb.2023.1189877

77. Doukyu N, Taguchi K. Involvement of catalase and superoxide dismutase in hydrophobic organic solvent tolerance of *Escherichia coli*. AMB Express. 2021;11:97; doi:10.1186/s13568-021-01258-w

78. Pinske C. The Ferredoxin-Like Proteins HydN and YsaA Enhance Redox Dye-Linked Activity of the Formate Dehydrogenase H Component of the Formate Hydrogenlyase Complex. Front Microbiol. 2018;9; doi:10.3389/fmicb.2018.01238

79. Panta PR, Doerrler WT. A link between pH homeostasis and colistin resistance in bacteria. Sci Rep. 2021;11:13230; doi:10.1038/s41598-021-92718-7

80. Vasilyev N, Liu MMJ, Epshtein V, Shamovsky I, Nudler E. General Transcription Factor from *E. coli* with a Distinct Mechanism of Action. bioRxiv. 2023;2023.09.17.558134; doi: 10.1101/2023.09.17.558134

81. Nasreen M, Purushothaman Nair R, Mcewan A, Kappler U. The Peptide Methionine Sulfoxide Reductase (MsrAB) of Haemophilus influenzae Repairs Oxidatively Damaged Outer Membrane and Periplasmic Proteins Involved in Nutrient Acquisition and Virulence. Antioxidants. 2022;11:1557; doi:10.3390/antiox11081557

82. Yuan J, Jin F, Glatter T, Sourjik V. Osmosensing by the bacterial PhoQ/PhoP two-component system. Proceedings of the National Academy of Sciences. 2017;114:E10792–8; doi:10.1073/pnas.1717272114

83. Steinsiek S, Stagge S, Bettenbrock K. Analysis of *Escherichia coli* mutants with a linear respiratory chain. PLoS One. 2014;9(1):e87307; doi:10.1371/journal.pone.0087307.

84. Akinori K, Hiroyuki T, Ryutaro U. Molecular Characterization of the PhoP-PhoQ Two-Component System in *Escherichia coli* K-12: Identification of Extracellular Mg2+-Responsive Promoters. J Bacteriol. 1999;181:5516–20; doi:10.1128/jb.181.17.5516-5520.1999

85. Podlesek Z, Žgur Bertok D. The DNA Damage Inducible SOS Response Is a Key Player in the Generation of Bacterial Persister Cells and Population Wide Tolerance. Front Microbiol .2020;11; doi:10.3389/fmicb.2020.01785

86. Bitoun JP, Wu G, Ding H. *Escherichia coli* FtnA acts as an iron buffer for re-assembly of iron–sulfur clusters in response to hydrogen peroxide stress. BioMetals. 2008;21:693–703; doi:10.1007/s10534-008-9154-7

87. C BD, J TR. Small Multidrug Resistance Protein EmrE Reduces Host pH and Osmotic Tolerance to Metabolic Quaternary Cation Osmoprotectants. J Bacteriol. 2012;194:5941–8; doi:10.1128/jb.00666-12

88. M FE, E EK, N GL, R GE, M MJ, C MA, et al. YfdW and YfdU Are Required for Oxalate-Induced Acid Tolerance in *Escherichia coli* K-12. J Bacteriol. 2013;195:1446–55; doi:10.1128/jb.01936-12

89. Ralph ET, Guest JR, Green J. Altering the anaerobic transcription factor FNR confers a hemolytic phenotype on *Escherichia coli* K12. Proceedings of the National Academy of Sciences. 1998;95:10449–52; doi:10.1073/pnas.95.18.10449

90. Wang X, Kim Y, Ma Q, Hong SH, Pokusaeva K, Sturino JM, et al. Cryptic prophages help bacteria cope with adverse environments. Nat Commun. 2010;1:147; doi:10.1038/ncomms1146

91. Barabote RD, Rendulic S, Schuster SC, Saier MH. Comprehensive analysis of transport proteins encoded within the genome of *Bdellovibrio bacteriovorus*. Genomics . 2007;90:424–46; doi:10.1016/j.ygeno.2007.06.002

92. Wang J, Ma W, Wang X. Insights into the structure of *Escherichia coli* outer membrane as the target for engineering microbial cell factories. Microb Cell Fact. 2021;20:73; doi:10.1186/s12934-021-01565-8

93. Gurmu D, Lu J, Johnson KA, Nordlund P, Holmgren A, Erlandsen H. The crystal structure of the protein YhaK from *Escherichia coli* reveals a new subclass of redox sensitive enterobacterial bicupins. Proteins: Structure, Function, and Bioinformatics. 2009;74:18–31; doi:10.1002/prot.22128

94. Outten CE, Outten FW, O'Halloran T V. DNA Distortion Mechanism for Transcriptional Activation by ZntR, a Zn(II)-responsive MerR Homologue in *Escherichia coli*. Journal of Biological Chemistry. 1999;274:37517–24; doi:10.1074/jbc.274.53.37517

95. Akbar S, Bhakta S, Sengupta J. Structural insights into the interplay of protein biogenesis factors with the 70S ribosome. Structure. 2021;29:755-767.e4; doi:10.1016/j.str.2021.03.005

96. K VDT, J TL, A CK, L SP, Sima SF. Characterization of the *Escherichia coli* AaeAB Efflux Pump: a Metabolic Relief Valve? J Bacteriol. 2004;186:7196–204; doi:10.1128/jb.186.21.7196-7204.2004

97. Bak G, Lee J, Suk S, Kim D, Young Lee J, Kim K, et al. Identification of novel sRNAs involved in biofilm formation, motility and fimbriae formation in *Escherichia coli*. Sci Rep. 2015;5:15287; doi:10.1038/srep15287

98. P DM, Chi-Fang W, Liang W, J VJ, E BW. DNA Microarray-Based Identification of Genes Controlled by Autoinducer 2-Stimulated Quorum Sensing in *Escherichia coli*. J Bacteriol. 2001;183:5239–47; doi:10.1128/jb.183.18.5239-5247.2001

99. Filenko N, Spiro S, Browning DF, Squire D, Overton TW, Cole J, Constantinidou C. The NsrR regulon of *Escherichia coli* K-12 includes genes encoding the hybrid cluster protein and the periplasmic, respiratory nitrite reductase. J Bacteriol. 2007;189:1203–9; doi:10.1128/jb.00080-07.

100. Khil PP, Camerini-Otero RD. Over 1000 genes are involved in the DNA damage response of *Escherichia coli*. Mol Microbiol. 2002;44:89–105; doi:10.1046/j.1365-2958.2002.02878.x

101. Erol I, Jeong K-C, Baumler DJ, Vykhodets B, Ho Choi S, Kaspar CW. H-NS controls metabolism and stress tolerance in *Escherichia coli* O157:H7 that influence mouse passage. BMC Microbiol. 2006;6:72; doi:10.1186/1471-2180-6-72

102. Zheng L. Catalytic mechanism and function evolvement studies of phosphatases within the haloacid dehalogenase superfamily (HADSF) [dissertation]. Albuquerque (NM): University of New Mexico; 2013. Available from: https://digitalrepository.unm.edu/chem_etds/31.

103. Born TL, Blanchard JS. Structure/function studies on enzymes in the diaminopimelate pathway of bacterial cell wall biosynthesis. Curr Opin Chem Biol. 1999;3:607–13; doi:10.1016/S1367-5931(99)00016-2

104. Hor L, Dobson RCJ, Downton MT, Wagner J, Hutton CA, Perugini MA. Dimerization of Bacterial Diaminopimelate Epimerase Is Essential for Catalysis. J Biol Chem . 2013;288:9238–48

105. Iyer LM, Leipe DD, Koonin E V, Aravind L. Evolutionary history and higher order classification of AAA+ ATPases. J Struct Biol. 2004;146:11–31; doi:

106. Luttringer F, Mulliez E, Dublet B, Lemaire D, Fontecave M. The Zn center of the anaerobic ribonucleotide reductase from *E. coli*. JBIC Journal of Biological Inorganic Chemistry . 2009;14:923–33; doi:10.1007/s00775-009-0505-9

107. Panta PR, Doerrler WT. A link between pH homeostasis and colistin resistance in bacteria. Sci Rep. 2021;11:13230; doi:10.1038/s41598-021-92718-7

108. Dapa T, Fleurier S, Bredeche M-F, Matic I. The SOS and RpoS Regulons Contribute to Bacterial Cell Robustness to Genotoxic Stress by Synergistically Regulating DNA Polymerase Pol II. Genetics. 2017;206:1349–60; doi:10.1534/genetics.116.199471

109. Passariello C, Forleo C, Micheli V, Schippa S, Leone R, Mangani S, et al. Biochemical characterization of the class B acid phosphatase (AphA) of *Escherichia coli* MG1655. Biochimica et Biophysica Acta (BBA) - Proteins and Proteomics. 2006;1764:13–9; doi:10.1016/j.bbapap.2005.08.028

110. Chen SH, Byrne RT, Wood EA, Cox MM. *Escherichia coli rad* gene: a novel function involved in radiation resistance and double-strand break repair. Mol Microbiol. 2015;95:754–68; doi:10.1111/mmi.12885

111. Chuang SE, Blattner FR. Characterization of twenty-six new heat shock genes of *Escherichia coli*. J Bacteriol. 1993;175:5242–52; doi:10.1128/jb.175.16.5242-5252.1993

112. Manganelli R, Gennaro ML. Protecting from Envelope Stress: Variations on the Phage-Shock-Protein Theme. Trends Microbiol. 2017;25:205–16; doi:10.1016/j.tim.2016.10.001

113. Freeman ZN, Dorus S, Waterfield NR. The KdpD/KdpE Two-Component System: Integrating K+ Homeostasis and Virulence. PLoS Pathog. 2013;9:e1003201-; doi:10.1371/journal.ppat.1003201

114. Meadows JA, Wargo MJ. Carnitine in bacterial physiology and metabolism. Microbiology (N Y). 2015;161:1161–74; doi:10.1099/mic.0.000080

115. Kolata P, Efremov RG. Structure of *Escherichia coli* respiratory complex I reconstituted into lipid nanodiscs reveals an uncoupled conformation. Swartz KJ, Carter AP, Kumar V, Letts JA, editors. Elife. 2021;10:e68710; doi:10.7554/eLife.68710

116. Korea C-G, Badouraly R, Prevost M-C, Ghigo J-M, Beloin C. *Escherichia coli* K-12 possesses multiple cryptic but functional chaperone–usher fimbriae with distinct surface specificities. Environ Microbiol. 2010;12:1957–77; doi:10.1111/j.1462-2920.2010.02202.x

117. Fu H, Lee J, Wang T. Heat-shock increases rpoD-dependent β-galactosidase activity in the *Escherichia coli* strains BD792 and B23. 2015;19

118. Gagarinova A, Hosseinnia A, Rahmatbakhsh M, Istace Z, Phanse S, Moutaoufik MT, et al. Auxotrophic and prototrophic conditional genetic networks reveal the rewiring of transcription factors in *Escherichia coli*. Nat Commun. 2022;13:4085; doi:10.1038/s41467-022-31819-x

119. Prusiner S, Davis JN, Stadtman ER. Regulation of glutaminase B in *Escherichia coli*. I. Purification, properties, and cold lability. Journal of Biological Chemistry. 1976;251:3447–56; doi: 10;251(11):3447-56

120. Iacometti C, Marx K, Hönick M, Biletskaia V, Schulz-Mirbach H, Satanowski A, et al. Activating silent glycolysis bypasses *Escherichia coli*; bioRxiv. 2021;2021.11.18.468982; doi: 10.34133/2022/9859643

121. Njenga R, Boele J, Öztürk Y, Koch H-G. Coping with stress: How bacteria fine-tune protein synthesis and protein transport. Journal of Biological Chemistry. 2023;299:105163; doi:10.1016/j.jbc.2023.105163

122. Hajra D, Nair AV, Chakravortty D. An elegant nano-injection machinery for sabotaging the host: Role of Type III secretion system in virulence of different human and animal pathogenic bacteria. Phys Life Rev. 2021;38:25–54; doi:10.1016/j.plrev.2021.05.007

123. Peek J, Christendat D. The shikimate dehydrogenase family: Functional diversity within a conserved structural and mechanistic framework. Arch Biochem Biophys. 2015;566:85–99; doi:10.1016/j.abb.2014.12.006

124. Miwa T, Taguchi H. *Escherichia coli* small heat shock protein IbpA plays a role in regulating the heat shock response by controlling the translation of σ32. Proceedings of the National Academy of Sciences. 2023;120:e2304841120; doi:10.1073/pnas.2304841120

125. Brocklehurst KR, Hobman JL, Lawley B, Blank L, Marshall SJ, Brown NL, et al. ZntR is a Zn(II)-responsive MerR-like transcriptional regulator of zntA in *Escherichia coli*. Mol Microbiol. 1999;31:893–902; doi: 10.1046/j.1365-2958.1999.01229.x

126. T CP. A Galvanizing Story—Protein Stability and Zinc Homeostasis. J Bacteriol. 2007;189:2953–4; doi:10.1128/jb.00173-07

127. Iannuzzi C, Adrover M, Puglisi R, Yan R, Temussi PA, Pastore A. The role of zinc in the stability of the marginally stable IscU scaffold protein. Protein Sci. 2014;23(9):1208-1219. doi:10.1002/pro.2501.

128. Joly N, Engl C, Jovanovic G, Huvet M, Toni T, Sheng X, et al. Managing membrane stress: the phage shock protein (Psp) response, from molecular mechanisms to physiology. FEMS Microbiol Rev. 2010;34:797–827; 10.1111/j.1574-6976.2010.00240.x

129. LeRoux M, Culviner PH, Liu YJ, Littlehale ML, Laub MT. Stress Can Induce Transcription of Toxin-Antitoxin Systems without Activating Toxin. Mol Cell. 2020;79:280-292.e8; doi:10.1016/j.molcel.2020.05.028

130. Flores-Kim J, Darwin AJ. The Phage Shock Protein Response. Annu Rev Microbiol. 2016;70:83–101; doi:10.1146/annurev-micro-102215-095359

131. Walsh P, Bursać D, Law YC, Cyr D, Lithgow T. The J-protein family: modulating protein assembly, disassembly and translocation. EMBO Rep. 2004;5:567-571–571; doi:10.1038/sj.embor.7400172

132. Park DM, Akhtar MdS, Ansari AZ, Landick R, Kiley PJ. The Bacterial Response Regulator ArcA Uses a Diverse Binding Site Architecture to Regulate Carbon Oxidation Globally. PLoS Genet. 2013;9:e1003839; doi:10.1371/journal.pgen.1003839

133. Anand A, Patel A, Chen K, Olson CA, Phaneuf P V, Lamoureux C, et al. Laboratory evolution of synthetic electron transport system variants reveals a larger metabolic respiratory system and its plasticity. Nat Commun. 2022;13:3682; 10.1038/s41467-022-30877-5

134. Henry C, Loiseau L, Vergnes A, Vertommen D, Mérida-Floriano A, Chitteni-Pattu S, et al. Redox controls RecA protein activity via reversible oxidation of its methionine residues. Kowalczykowski SC, Storz G, editors. Elife. 2021;10:e63747; doi:10.7554/eLife.63747

135. Flint DH, Emptage MH, Guest JR. Fumarase A from *Escherichia coli:* purification and characterization as an iron-sulfur cluster containing enzyme. Biochemistry . 1992;31:10331–7; doi:10.1021/bi00157a022

136. Park S-J, Tseng C-P, Gunsalus RP. Regulation of succinate dehydrogenase (sdhCDAB) operon expression in *Escherichia coli* in response to carbon supply and anaerobiosis: role of ArcA and Fnr. Mol Microbiol. 1995;15:473–82; doi:10.1111/j.1365-2958.1995.tb02261.x

137. Roth M, Jaquet V, Lemeille S, Bonetti E-J, Cambet Y, Francois P, et al. Transcriptomic Analysis of *E. coli* after Exposure to a Sublethal Concentration of Hydrogen Peroxide Revealed a Coordinated Up-Regulation of the Cysteine Biosynthesis Pathway. Antioxidants. 2022;11; doi:10.3390/antiox11040655

138. Friedrich T, Dekovic DK, Burschel S. Assembly of the *Escherichia coli* NADH:ubiquinone oxidoreductase (respiratory complex I). Biochimica et Biophysica Acta (BBA) - Bioenergetics. 2016;1857:214–23; doi:10.1016/j.bbabio.2015.12.004

139. Prasad I, Young B, Schaefler S. Genetic Determination of the Constitutive Biosynthesis of Phospho-β-Glucosidase A in *Escherichia coli* K-12. J Bacteriol. 1973;114:909–15. 10.1128/jb.114.3.909-915.1973

140. Kuznetsova E, Proudfoot M, Gonzalez CF, Brown G, Omelchenko M V, Borozan I, et al. Genome-wide Analysis of Substrate Specificities of the *Escherichia coli* Haloacid Dehalogenase-like Phosphatase Family*. Journal of Biological Chemistry. 2006;281:36149–61; doi:10.1074/jbc.m605449200

141. Sobota JM, Imlay JA. Iron enzyme ribulose-5-phosphate 3-epimerase in *Escherichia coli* is rapidly damaged by hydrogen peroxide but can be protected by manganese. Proceedings of the National Academy of Sciences. 2011;108:5402–7; doi:10.1073/pnas.1100410108

142. Chuanboon K, Na Nakorn P, Pannengpetch S, Laengsri V, Nuchnoi P, Isarankura-Na-Ayudhya C, et al. Proteomics and bioinformatics analysis reveal potential roles of cadmium-binding proteins in cadmium tolerance and accumulation of *Enterobacter cloacae*; PeerJ. 2019;7:e6904; https://pubmed.ncbi.nlm.nih.gov/31534833/

143. Imlay JA, Linn S. Bimodal pattern of killing of DNA-repair-defective or anoxically grown *Escherichia coli* by hydrogen peroxide. J Bacteriol. 1986;166:519–27; doi:10.1128/jb.166.2.519-527.1986

144. McCarthy DJ, Smyth GK. Testing significance relative to a fold-change threshold is a TREAT. Bioinformatics. 2009;25:765–71; doi:10.1093/bioinformatics/btp053

145. Umbarger HE, Brown B. Threonine deamination in *Escherichia coli*. II. Evidence for two L-threonine deaminases. J Bacteriol. 1957;73(1):105–12; doi:10.1128/jb.73.1.105-112.1957.

146. Julien M, Elisa G, Ronald VE, Enrique TMO, Ladan K, Laleh K, et al. Gene Erosion Can Lead to Gain-of-Function Alleles That Contribute to Bacterial Fitness. mBio. 2021;12:10.1128/mbio.01129-21; doi:10.1128/mbio.01129-21

147. Greenfield D, McEvoy AL, Shroff H, Crooks GE, Wingreen NS, Betzig E, et al. Self-Organization of the *Escherichia coli* Chemotaxis Network Imaged with Super-Resolution Light Microscopy. PLoS Biol. 2009;7:e1000137; doi:10.1371/journal.pbio.1000137

148. Guinote IB, Moreira RN, Barahona S, Freire P, Vicente M, Arraiano CM. Breaking through the stress barrier: the role of BolA in Gram-negative survival. World J Microbiol Biotechnol. 2014;30:2559–66; 10.1007/s11274-014-1702-4

149. Hemm MR, Paul BJ, Miranda-Ríos J, Zhang A, Soltanzad N, Storz G. Small stress response proteins in *Escherichia coli*: proteins missed by classical proteomic studies. J Bacteriol. 2010;192(1):46–58; doi:10.1128/JB.00872-09.

150. J RB, H DR, E PR, L SH, I BP, Aindrila M, et al. Functional Genomic Study of Exogenous n-Butanol Stress in *Escherichia coli*. Appl Environ Microbiol. 2010;76:1935–45; doi:10.1128/AEM.02323-09

151. Chen B, Chu T-W, Chiu K, Hong M-C, Wu T-M, Ma J-W, et al. Transcriptomic analysis elucidates the molecular processes associated with hydrogen peroxide-induced diapause termination in Artemia-encysted embryos. PLoS One. 2021;16:e0247160; doi:10.1371/journal.pone.0247160

152. Allison H, Jacquelyn S, Alexandra K, Kathleen C, Matthew Y, Dennis W, et al. The Bacterial iprA Gene Is Conserved across Enterobacteriaceae, Is Involved in Oxidative Stress Resistance, and Influences Gene Expression in *Salmonella enterica* Serovar Typhimurium. J Bacteriol. 2016;198:2166–79; doi:10.1128/jb.00144-16

153. Martínez Y, Li X, Liu G, Bin P, Yan W, Más D, et al. The role of methionine on metabolism, oxidative stress, and diseases. Amino Acids. 2017;49:2091–8; doi:10.1007/s00726-017-2494-2

154. Clausznitzer D, Oleksiuk O, Løvdok L, Sourjik V, Endres RG. Chemotactic Response and Adaptation Dynamics in *Escherichia coli*. PLoS Comput Biol. 2010;6:e1000784; doi:10.1371/journal.pcbi.1000784

155. Bouillet S, Hamdallah I, Majdalani N, Tripathi A, Gottesman S. A negative feedback loop is critical for recovery of RpoS after stress in Escherichia coli. bioRxiv. 2023;2023.11.09.566509; doi:10.1101/2023.11.09.566509.

156. Song S, Wood TK. A primary physiological role of toxin/antitoxin systems is phage inhibition. Front Microbiol. 2020;11:1895; doi:10.3389/fmicb.2020.01895.

157. chmidt M, Proctor T, Diao R, Freddolino PL. *Escherichia coli* YigI is a conserved Gammaproteobacterial acyl-CoA thioesterase permitting metabolism of unusual fatty acid substrates. J Bacteriol. 2022;204:e00014-22; doi:10.1128/JB.00014-22.

158. Jack RL, Sargent F, Berks BC, Sawers G, Palmer T. Constitutive expression of *Escherichia coli* tat genes indicates an important role for the twin-arginine translocase during

aerobic and anaerobic growth. J Bacteriol. 2001;183(5):1801–4; doi:10.1128/jb.183.5.1801-1804.2001.

159. Zhao R, Li Z, Sun Y, Ge W, Wang M, Liu H, et al. Engineered *Escherichia coli* Nissle 1917 with urate oxidase and an oxygen-recycling system for hyperuricemia treatment. Gut Microbes. 2022;14:2070391; doi:10.1080/19490976.2022.2070391

160. Hryniewicz M, Sirko A, Pałucha A, Böck A, Hulanicka D. Sulfate and thiosulfate transport in *Escherichia coli* K-12: identification of a gene encoding a novel protein involved in thiosulfate binding. J Bacteriol. 1990;172(6):3358–66; doi:10.1128/jb.172.6.3358-3366.1990.

161. Sayers EW, Bolton EE, Brister JR, Canese K, Chan J, Comeau DC, et al. Database resources of the National Center for Biotechnology. 2022; doi:10.1093/nar/gkab1112

162. Krueger F, James F, Ewels P, Afyounian E, Weinstein M, Schuster-Boeckler B, et al. FelixKrueger/TrimGalore: v0.6.10 - add default decompression path. Zenodo; 2023; doi:10.5281/zenodo.7598955

163. FastQC. 2015. Available from: https://qubeshub.org/resources/fastqc

164. Langmead B, Salzberg SL. Fast gapped-read alignment with Bowtie 2. Nat Methods. 2012;9:357–9; doi:10.1038/nmeth.1923

165. Wang L, Wang S, Li W. RSeQC: quality control of RNA-seq experiments. Bioinformatics. 2012;28:2184–5; doi:10.1093/bioinformatics/bts356

166. Liao Y, Smyth GK, Shi W. featureCounts: an efficient general purpose program for assigning sequence reads to genomic features. Bioinformatics. 2014;30:923–30; doi:10.1093/bioinformatics/btt656

167. Ewels P, Magnusson M, Lundin S, Käller M. MultiQC: summarize analysis results for multiple tools and samples in a single report. Bioinformatics. 2016;32:3047–8. Available from: https://doi.org/10.1093/bioinformatics/btw354

168. Lamoureux CR, Decker KT, Sastry A V, Rychel K, Gao Y, McConn JL, et al. A multi-scale expression and regulation knowledge base for *Escherichia coli*. Nucleic Acids Res. 2023;51:10176–93; doi:10.1093/nar/gkad750

169. Consortium TGO, Aleksander SA, Balhoff J, Carbon S, Cherry JM, Drabkin HJ, et al. The Gene Ontology knowledgebase in 2023. Genetics. 2023;224:iyad031; doi:10.1093/genetics/iyad031

170. Gumienny R. GEOparse: Python Library to Access Gene ExpressionOmnibus Database(GEO). Available from: https://pypi.org/project/GEOparse/

171. Kim D, Seo SW, Gao Y, Nam H, Guzman GI, Cho B-K, et al. Systems assessment of transcriptional regulation on central carbon metabolism by Cra and CRP. Nucleic Acids Res . 2018;46:2901–17; doi:10.1093/nar/gky069

172. Spearman Rank Correlation Coefficient. The Concise Encyclopedia of Statistics. New York, NY: Springer New York; 2008. p. 502–5. Available from: https://doi.org/10.1007/978-0-387-32833-1_379

173. Martelli PL, Fariselli P, Casadio R. An ENSEMBLE machine learning approach for the prediction of all-alpha membrane proteins. Bioinformatics. 2003;19:i205–11. ; doi:10.1093/bioinformatics/btg1027

174. Pierleoni A, Martelli PL, Fariselli P, Casadio R. BaCelLo: a balanced subcellular localization predictor. Bioinformatics. 2006;22:e408–16; doi:10.1093/bioinformatics/btl222

175. Pierleoni A, Martelli PL, Casadio R. PredGPI: a GPI-anchor predictor. BMC Bioinformatics. 2008;9:392; doi:10.1186/1471-2105-9-392

176. Pierleoni A, Martelli PL, Casadio R. MemLoci: predicting subcellular localization of membrane proteins in eukaryotes. Bioinformatics. 2011;27:1224–30; doi:10.1093/bioinformatics/btr108

177. Savojardo C, Fariselli P, Casadio R. BETAWARE: a machine-learning tool to detect and predict transmembrane beta-barrel proteins in prokaryotes. Bioinformatics . 2013;29:504–5; doi:10.1093/bioinformatics/bts728

178. Szklarczyk D, Gable AL, Nastou KC, Lyon D, Kirsch R, Pyysalo S, et al. The STRING database in 2021: customizable protein–protein networks, and functional characterization of user-uploaded gene/measurement sets. Nucleic Acids Res. 2021;49:D605–12; 10.1093/nar/gkaa1074

179. Fernando PC, Mabee PM, Zeng E. Integration of anatomy ontology data with protein–protein interaction networks improves the candidate gene prediction accuracy for anatomical entities. BMC Bioinformatics. 2020;21:442; doi:10.1186/s12859-020-03773-2

180. Remmert M, Biegert A, Hauser A, Söding J. HHblits: lightning-fast iterative protein sequence searching by HMM-HMM alignment. Nat Methods. 2012;9:173–5; doi:10.1038/nmeth.1818

181. Bagheri H, Dyer R, Severin A, Rajan H. Comprehensive Analysis of Non Redundant Protein Database. 2020; doi:10.21203/rs.3.rs-54568/v1

182. Andreeva A, Kulesha E, Gough J, Murzin AG. The SCOP database in 2020: expanded classification of representative family and superfamily domains of known protein structures. Nucleic Acids Res. 2020;48:D376–82. Available from:10.1093/nar/gkz1064

183. Barrio-Hernandez I, Yeo J, Jänes J, Mirdita M, Gilchrist CLM, Wein T, et al. Clustering predicted structures at the scale of the known protein universe. Nature. 2023;622:637–45; doi:10.1038/s41586-023-06510-w

184. Tuttle AR, Trahan ND, Son MS. Growth and Maintenance of *Escherichia coli* Laboratory Strains. Curr Protoc. 2021;1:e20; doi:10.1002/cpz1.20

185. Schroeder A, Mueller O, Stocker S, Salowsky R, Leiber M, Gassmann M, et al. The RIN: an RNA integrity number for assigning integrity values to RNA measurements. BMC Mol Biol. 2006;7:3; doi:10.1186/1471-2199-7-3

186. Lataretu M, Hölzer M. RNAflow: An Effective and Simple RNA-Seq Differential Gene Expression Pipeline Using Nextflow. Genes (Basel). 2020;11:1487; doi:10.3390/genes11121487

187. Chen S, Zhou Y, Chen Y, Gu J. fastp: an ultra-fast all-in-one FASTQ preprocessor. Bioinformatics. 2018;34:i884–90; doi:10.1093/bioinformatics/bty560

188. Chen S, Zhou Y, Chen Y, Gu J. fastp: an ultra-fast all-in-one FASTQ preprocessor. Bioinformatics. 2018;34:i884–90; doi:10.1093/bioinformatics/bty560

189. Kim D, Langmead B, Salzberg SL. HISAT: a fast spliced aligner with low memory requirements. Nat Methods. 2015;12:357–60; doi:10.1038/nmeth.3317

190. Li H, Handsaker B, Wysoker A, Fennell T, Ruan J, Homer N, et al. The Sequence Alignment/Map format and SAMtools. Bioinformatics. 2009;25:2078–9.; doi:10.1093/bioinformatics/btp352

191. Liao Y, Smyth GK, Shi W. featureCounts: an efficient general purpose program for assigning sequence reads to genomic features. Bioinformatics. 2014;30:923–30; doi:10.1093/bioinformatics/btt656

192. Love MI, Huber W, Anders S. Moderated estimation of fold change and dispersion for RNA-seq data with DESeq2. Genome Biol. 2014;15:550; doi:10.1186/s13059-014-0550-8

193. Duda JC, Drenda C, Kästel H, Rahnenführer J, Kappenberg F. Benefit of using interaction effects for the analysis of high-dimensional time-response or dose-response data for two-group comparisons. Sci Rep. 2023;13:20804; doi:10.1038/s41598-023-47057-0

194. Liou G-G, Chao Kaberdina A, Wang W-S, Kaberdin VR, Lin-Chao S. Combined Transcriptomic and Proteomic Profiling of *E. coli* under Microaerobic versus Aerobic Conditions: The Multifaceted Roles of Noncoding Small RNAs and Oxygen-Dependent Sensing in Global Gene Expression Control. Int J Mol Sci. 2022;23; doi:10.3390/ijms23052570